Mutations compensating for cell polarity defects change the gene-fitness relationship on a genome-wide scale

Enzo Kingma[a] **and Liedewij Laan**[a,1]

[a]Department of Bionanoscience, Kavli Institute of Nanoscience Delft, Delft University of Technology, Delft 2629 HZ, the Netherlands.; [1]To whom correspondence should be addressed. E-mail: L.Laan@tudelft.nl

Functional defects resulting from deleterious mutations can often be restored during evolution by compensatory mutations elsewhere in the genome. Importantly, this process can generate the molecular diversity seen in networks regulating the same biological function. How the capacity for compensatory evolution is embedded in the structure of biological networks is still unresolved. Here, we study a case in *Saccharomyces cerevisiae* where a genetic perturbation in a module related to polarity establishment is compensated by making additional gene deletions. A transposon mutagenesis screen revealed that compensatory evolution altered the gene-fitness relation of approximately 13% of the annotated genes. Interestingly, a nearly equal number of genes become more and less tolerant to disruptions, indicating substantial functional rewiring of genes. Grouping the affected genes by their biological function, we find that they are involved in a diverse set of processes, of which many have no clear link to cell polarity. Our results show that mutations compensating for defects in one functional module can have global consequences that influence the evolutionary direction of many other cellular processes.

1. Introduction

All cells must perform a series of complex tasks that allow them to survive and either replicate or remain dormant. The completion of these tasks, as well as their temporal regulation, is dependent on a dense network of proteins, DNA, RNA and other small molecules that interact physically. Using classical genetics in model organisms, the set of molecular events that need to take place in order to perform several biological functions has been uncovered, with hallmark examples being endocytocis (1, 2), cytokinesis (3) and cell polarization (4). While it is clear that there can be strong evolutionary conservation on the functional and molecular level (5), examples are emerging where a protein that is essential for the proper execution in one species can be absent in other, closely related, species that perform the same biological function (6–8). In rare cases, this type of divergence is even seen between different individuals of the same species (9). Thus, two organisms that are capable of performing the same biological function may rely on different mechanisms to do so. Such examples that do not conform with the standard view of how these biological processes work in well studied species highlight that pathway composition can be flexible during evolution, even when the resulting phenotypes are similar. Evolving different mechanisms for the same biological function is tightly linked with the capacity to undergo compensatory evolution (10). During compensatory evolution, the negative effects of a mutation in one gene becomes buffered by mutations elsewhere in the genome (11, 12), a form of epistasis that is exploited by suppressor screens (13). In extreme cases, compensatory evolution can result in the loss of essential genes (14, 15). Although increasingly recognized as an important evolutionary mechanism that can drive evolutionary novelty (16–19), how the possibilities for compensation are related to the structure of biological interaction networks is still an open question.

A view that gained popularity at the beginning of this millennium and that has largely persisted is that biological networks tend to be organized in modules (20–23). That is, interaction networks can be divided into several smaller sub-networks that each relate to a particular biological function. Within the cell, these functional modules are combined to constitute different pathways. The evidence for modularity has been found in the successful *in vitro* reconstitution of several functional modules (24–26) and the ability to transplant them between different species (27, 28) or cell types(29). Importantly, modularity has been put forward as the major feature that makes networks evolvable (22, 30). Building a larger network from smaller building blocks that each regulate a single property allows each function to be optimized independently from others, which would promote evolvability by reducing the number of pleiotropic constraints (23). Thus, the idea of network modularity implies that the effects of compensatory mutations should be isolated to the module that was initially perturbed, or at least to closely connected modules. However, it is unclear whether this implication is correct, as the effects of evolution are rarely studied beyond those genes that acquire mutations. In addition, several studies have questioned the degree of modularity in biological networks and its possible role during evolution (31). For example, in networks that were artificially evolved in computer simulations, those with a non-modular design were often able to get closer to the optimal functionality than modular networks (32). Another computational study showed that networks with similar levels of architectural modularity can differ substantially in their evolvability (33). Finally, a study using phylogenetics demonstrated that the functional modules identified in a non-evolving network show surprisingly little conservation during evolution, seemingly contradicting the idea that modularity promotes evolvability by preventing cross-talk between modules (34).

To elucidate how the architecture of biological networks facilitates compensatory evolution and determine if modularity indeed plays a crucial role, cell polarity is an attractive biological function to focus on. On a functional level, cell polarity is highly conserved throughout the tree of life (35), yet the composition of the polarity network can not only differ between related species, but also between different strains of the same species (6, 36). In addition, the *in vitro* reconstitution of pattern forming systems (37–40), which encompass cell polarization mechanisms, suggests that the networks regulating the polarity pathway can be broken up into functional modules (figure 1a). In a recent study, it was shown that a nearly-essential component of the polarity network in budding yeast can be made dispensable during experimental evolution. Specifically, Laan et al. (41) synthetically deleted the polarity protein Bem1 in the yeast *Saccharomyces cerevisiae*, thereby breaking the feedback loop which current theory predicts to be the main driver of efficient cell polarization (42). While the loss of Bem1 drastically decreases fitness, nonsense mutations in two other genes (*BEM3* and *NRP1*) can recover fitness to near wild-type levels (figure 1b). In agreement with the idea that modules evolve independently of each other, Bem3 is a known component of the polarity network. The function of Nrp1 is currently unknown and may therefore have a yet to be determined role in polarity establishment. Importantly, these results provide an example for how the loss of a nearly essential gene can be facilitated by compensatory evolution. The finding that compensation requires only nonsense mutations suggests that a latent pathway for cell polarization exists that becomes active when the two genes are deleted.

The structure of this latent pathway and the mechanism through which its manifestation is achieved by compensatory gene deletions is currently unknown. Recent work based on mathematical modeling proposed a Bem1-independent mechanism for polarization that relies on redundancy within the polarity pathway (43), but has not been experimentally

verified. In this article, we search for the components of a latent pathway for cell polarity by identifying the genes that are affected by compensatory evolution through a transposon mutagenesis screen (figure 1c). Because polarity establishment is a crucial event in the cell cycle of *S. cerevisiae*, gene fitness, which we define as the fitness effect associated with loss of the gene, should increase for genes that play a role in the latent polarity pathway. Surprisingly, we find that the deletion of Bem1, Bem3 and Nrp1 affects the fitness of a substantial part ($\sim 13\%$) of the genome and we observe cases of both increased and decreased gene fitness scattered across several biological processes. Due to the size and diversity of this set of genes, we considered it unlikely that all these changes in gene fitness are related to the manifestation of a latent pathway for polarity establishment. In addition, while we were able to speculate on a possible structure of this latent pathway, the currently known interactions between these polarity proteins are insufficient to explain the changes in gene fitness we observe. We tested whether the observed gene fitness changes can be predicted from the structure of the protein-protein interaction network, but found no signs of any correlation with three commonly used network centralities. Overall, our data demonstrates that compensatory mutations occurring in response to the perturbation of a single functional module can globally alter the genotype-fitness relationship across many other modules. This finding suggests that the negative fitness effects of losing an important gene are mitigated by a global rewiring of the protein interaction network. Thus, even if modular structures are present in biological networks at any point in time, their role during evolution appears to be minor. Instead, our results indicate that compensatory evolution is a complex process that involves a large part of the network. The next challenge will be to uncover the rules dictating which genes are affected by compensatory mutations.

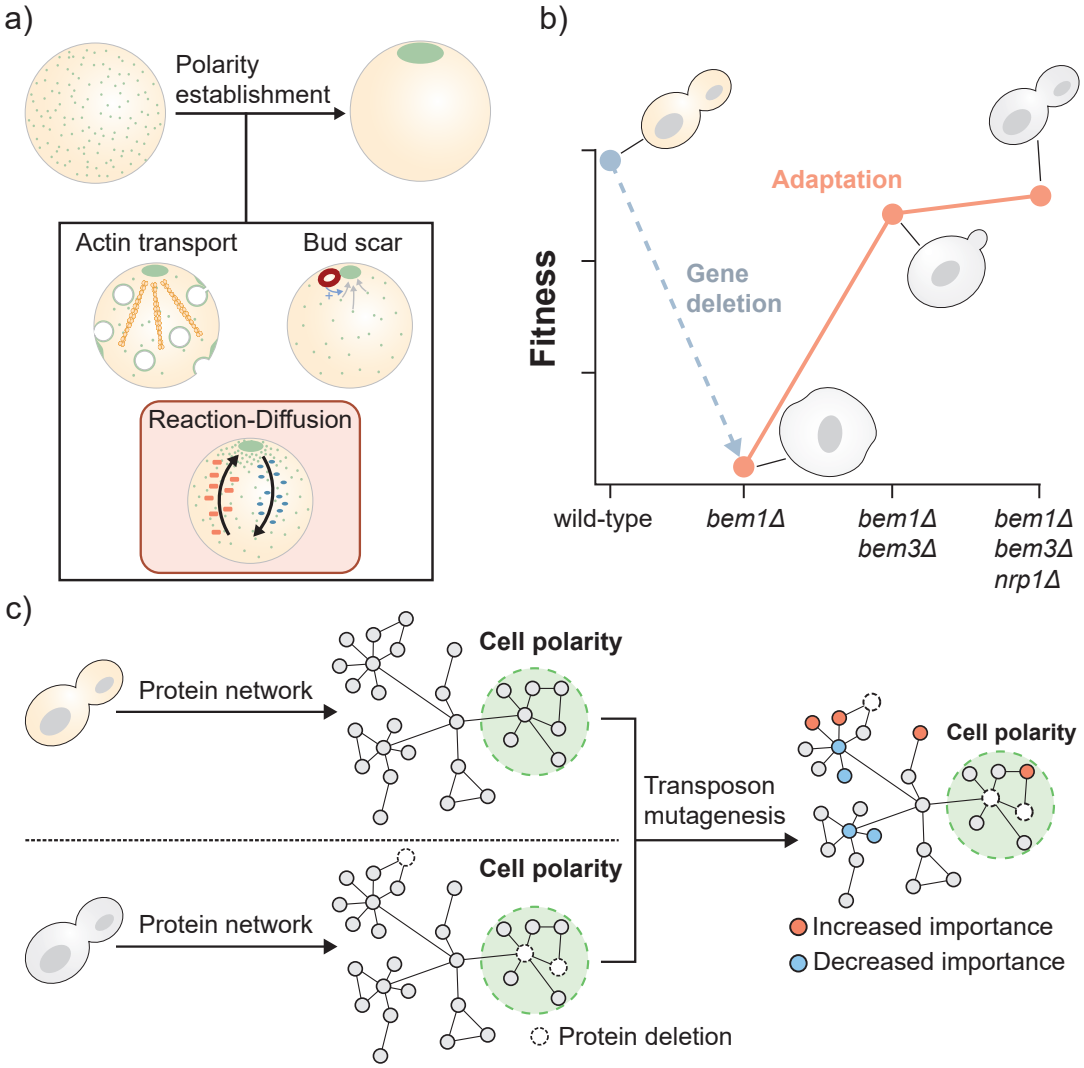

Fig. 1. Determining the consequences of compensatory evolution of the polarity module on global cellular physiology. (**a**) Polarity establishment is an evolutionary conserved function of nearly all cell types. In budding yeast, cell polarization is initiated by the formation of an asymmetric distribution of Cdc42 (shown in green). Endocytosis, exocytosis, spatial landmarks and a Bem1-mediated reaction-diffusion module have all been suggested to be involved in Cdc42 polarization dynamics. Here, we study the evolutionary response after genetically perturbing the reaction-diffusion module. (**b**) The phenotypic effects resulting from the deletion of the polarity protein Bem1 can be compensated by the additional loss of Bem3 and Nrp1. The resulting polarity mutant has a fitness similar to a wild-type strain under standard laboratory conditions. The figure is based on previous data obtained by Laan et al. (41). (**c**) We use transposon mutagenesis to determine the effects of compensatory evolution on the genotype-fitness relationship on a genome-wide scale. We expect that genes that display an altered relationship to cellular fitness between the wild-type strain and the polarity mutant are encoding for a protein that has taken on a different physiological role.

2. Results

A. Mutations compensating a genetic perturbation of the polarity network change gene fitness on a genome-wide scale. The finding that gene deletions are sufficient to largely restore cell polarization suggests that a latent pathway for polarity establishment exists. Somehow, the loss of Bem3 and Nrp1 promotes the activity of this latent pathway. We hypothesized that there are two possibilities for how gene loss might lead to pathway activation. The first is that the gene deletions allows other proteins to participate in novel interactions, for example because they now have a free binding site or a different localization pattern. Thus, polarization efficiency is restored because other proteins form an alternative pathway. Given that polarity establishment is a critical event for cell cycle progression in *S. cerevisiae*, we expect that the genes encoding for these proteins will have a stronger negative effect on fitness when deleted in the polarity mutant than when deleted in the wild-type strain. The second possibility is that the loss of Bem1 on one hand and the deletion of Bem3 and Nrp1 on the other have antagonistic effects on Cdc42 activity. That is, it represents a case where the loss of either an inhibitor or activator is deleterious, but deleting both simultaneously leads to a new equilibrium (44). If this is the case, the gene-fitness relationship should largely remain unchanged when Bem1, Bem3 and Nrp1 are deleted.

To distinguish between these two possibilities, we performed the transposon mutagenesis screen SATAY (45) in the wild-type strain and the polarity mutant. Briefly, SATAY allows us to estimate gene fitness on a genome-wide scale by measuring the effect of gene disruptions caused by the MiniDS transposon. Cells are propagated in media containing galactose to induce transposition, resulting in a saturated library of gene disruption mutants. After transposition, the cells are reseeded in rich media and allowed to grow until saturation. During this time frame, fitness differences become apparent as differences in relative mutant abundance. To estimate mutant abundance and thereby fitness, genomic DNA is extracted from the population and the transposon insertion sites are identified using a targeted sequencing approach. In this method, the insertion site serves as a tag by which each mutant can be identified and the number of reads mapping to each insertion site is taken to reflect the abundance of that mutant.

We generated a total of twelve SATAY libraries, of which six were made with the wild-type strain and six were made with the polarity mutant (figure 2a). To estimate gene fitness, we summed the read counts of the transposon insertion sites that map within each coding region. We corrected for a possible skew in the read count distribution and differences in sequencing depth between the libraries by first performing a Beta-geometric correction followed by a median of ratio normalization (see section A and figure S1). The six different replicates of each genetic background were then used to obtain the mean (μ) and variance (σ) of the summed read count distribution for each gene. The changes in gene fitness between the two genetic backgrounds are presented together with their significance level in the form of a volcano plot in figure 2b.

To our surprise, we found that at a significance level of 0.05 a large part of the genome has a differential fitness between the wild-type strain and the polarity mutant. In total, 883 genes (13% of all annotated coding regions) displayed an altered tolerance to transposon disruptions between the two strains (figure 2c). For comparison, we performed the same analysis with replicate libraries obtained from the same genetic background in a 3 vs. 3 fashion and found no significant differences (figure S2), although the statistical power is admittedly lower when comparing less replicates. Looking at the set of genes that fall below the significance threshold in more detail, we see that the number of genes with an increased gene fitness (414) and a decreased gene fitness (468) is approximately equal. Thus, the gene deletions do not simply result in a dependency on other genes to restore the perturbed function, but rather cause a reorganization of the gene-fitness relationship. Interestingly, this reorganization also affects a group of genes that have been annotated as essential by the Saccharomyces Genome Database (figure 2c).

Together, these results show that genetic compensation following the perturbation of a single module affects gene fitness on a genome-wide scale. The fact that we find both genes that are associated with cell polarization (for example, *SPA2*, *BNI1*, and *AXL2*) and those that lack any know connection to cell polarity (for example, *DYN1*, *CWP2*, and *MEC1*) demonstrates the global impact of compensatory evolution on cellular physiology. Furthermore, the nearly equal numbers of genes with increased and decreased fitness indicates that the compensatory gene deletions reshape the relative importance of cellular processes rather than lead to a decline in mutational robustness.

B. Changes in gene fitness cannot be predicted from the structure of the protein-protein interaction network. Are all genes equally likely to change their fitness during compensatory evolution? If not, understanding what determines this likelihood would provide opportunities for making evolutionary predictions. Classically, the physical interactions that take place within the cell are seen as the level of organization that connects genotype to phenotype. Various studies have indeed suggested a link between the role of a protein for the structure of the physical interaction network and the impact its loss has on organismal phenotype (46–49). For example, the likelihood of a protein being essential is often found to be related to the number of interaction partners a protein has (50). Thus, one would intuitively expect physical interaction networks to harbour relevant information for making evolutionary predictions. However,

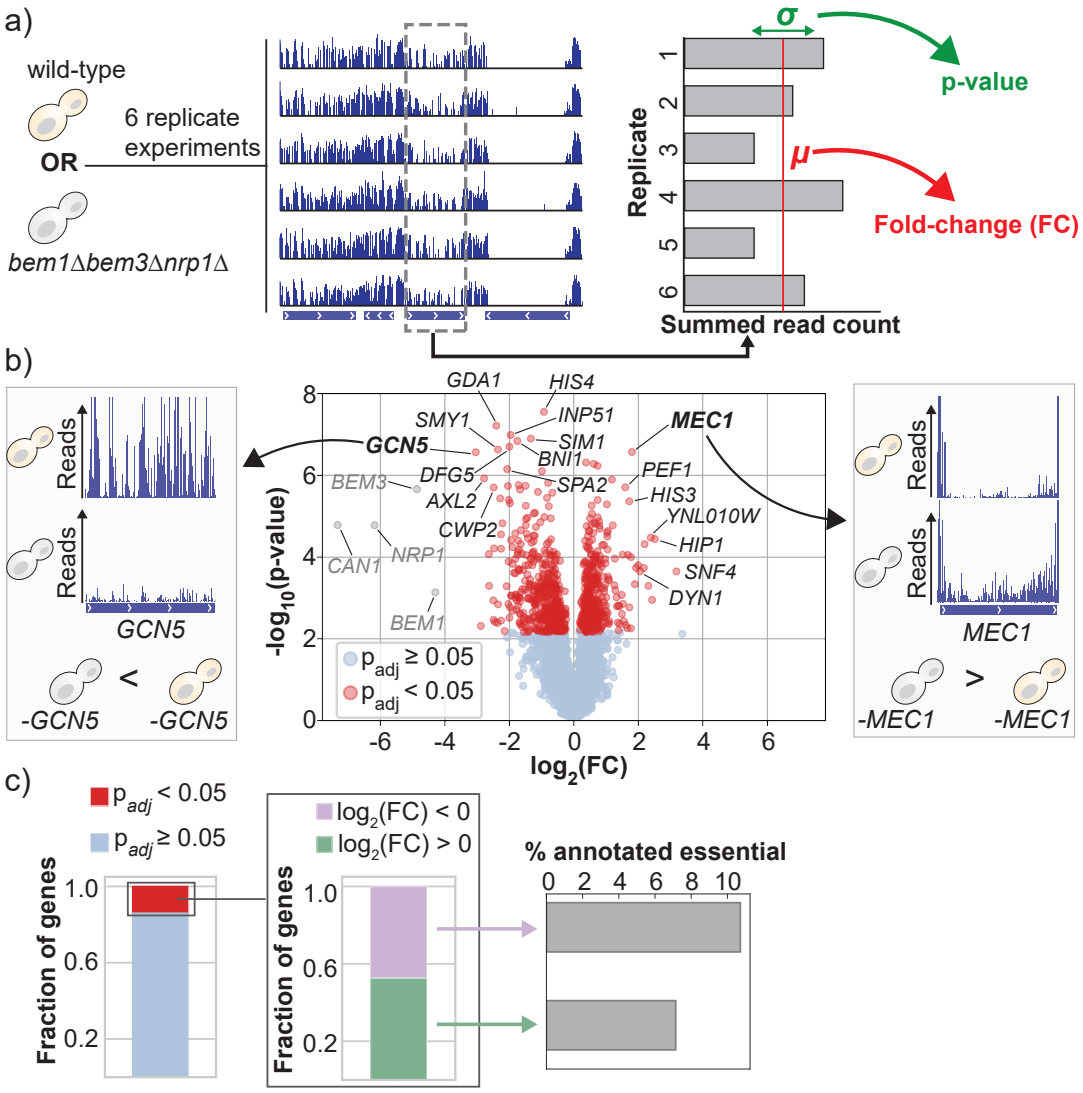

Fig. 2. Compensatory gene deletions change the gene-fitness relation of a large part of the genome. (**a**) We created six replicate SATAY libraries of the wild-type strain and six replicate libraries of the polarity mutant. To estimate gene fitness, we summed the read counts of transposon insertions that map to the same coding region. The mean μ and variance σ of the read sums for each gene was determined from the six replicate libraries of each genetic background. The mean and variance were subsequently used to determine the fold-change and significance level of the difference in summed read counts between the two genetic backgrounds. (**b**) Volcano plot of the changes in gene fitness showing the log fold-change (FC) and the significance value of the differences in gene fitness between the two strains. Positive log fold-changes relate to genes that have a higher fitness in the polarity mutant relative to the wild-type strain. Statistical significance was determined with Welch's t-test and corrected for multiple hypothesis testing with the Benjamini-Hochberg procedure. Genes that have been grayed out correspond to genes that were synthetically deleted from the genome of the polarity mutant during strain construction. (**c**) Approximately 13% of all annotated genes display a significantly altered tolerance to transposon disruptions between the two strains. An analysis of the sign of gene fitness changes in this set of genes shows that the ratio of genes that increase their relative fitness and those that decrease their relative fitness in the polarity mutant is nearly equal. Both the set of genes with increased and decreased fitness includes several genes that have been annotated as essential.

whether a correlation exists between a protein's topological properties in the physical interaction network and the likelihood that gene fitness changes during evolution has not yet been studied.

To evaluate the potential use of physical interaction networks for predicting gene fitness changes, we constructed a protein-protein interaction (PPI) network for the proteome of *S. cerevisiae*. Protein interactions were taken from the Multi-Validated dataset available from the BioGRID (51, 52). Here, Multi-Validated signifies that an interaction is only assigned if it has been reported by at least two different publication sources or experimental systems. Because this includes interactions that have been identified using high-throughput *in vitro* measurements, the network represents protein interactions that can take place in some environments, but do not necessarily do so *in vivo*. The resulting PPI network consists of 3799 proteins (nodes) and 17205 undirected interactions (edges) and is shown in figure 3a. The large majority of these proteins can be grouped into a single fully connected graph, and only few proteins are disconnected. However, we note that this PPI network is inherently incomplete, as it contains only 65% of the estimated total 5800 proteins in the yeast proteome. Unfortunately, one of our deleted proteins (Nrp1) is among those that are absent in the PPI network, which is most likely a consequence of Nrp1 being an understudied protein. Despite being incomplete, we were still able to validate the existence of the centrality-lethality rule (50) in our constructed network (figure 3b-c). We therefore considered this incomplete network to still contain the major structural features of the true PPI network.

The topological properties of a node in a network can be described using metrics that are collectively known as centralities. These centralities indicate the relative importance of a node for maintaining different aspects of network architecture (53). For example, the loss of a node with a high degree centrality will have a large impact on the connectedness of the network. Here, we focus on the three most commonly used centralities: degree, betweenness and closeness. The distributions of these three centralities in our constructed PPI network are shown in figure S3b-d. We find that the degree distribution in our network (figure S3b) follows the sub-linear dependency on a log-log scale that is characteristic for biological networks (54–56). Furthermore, when we annotated the centralities of four proteins related to polarity establishment, Bem1, Bem2, Bem3 and Cdc42, we found that proteins with a high (Bem1 and Cdc42) and those with a low (Bem2 and Bem3) fitness impact when lost could be grouped by their degree and betweenness values, but not by their closeness.

Next, we looked for a correlation between these three centralitities and the probability that the protein is encoded by a gene with a differential fitness between the two genetic backgrounds (figure 4). For all centralities tested here, the probability distribution was uniform, indicating that there is no dependency on these PPI network centralities. These results suggest that the structure of the PPI network we generated does not allow prediction of which genes will be affected by compensatory mutations.

C. Clustering of a functional association network reveals the different biological processes affected by compensatory mutations. We were unable to identify a relation between the PPI network structure and the set of genes that we found to be affected by compensatory evolution. However, contributing to the same physiological process does not require two proteins to interact physically. Some functional organization may therefore still exists within the set of genes we identified to have a significantly differential fitness. We therefore attempted to capture the possible functional relation between our genes using a functional association network.

We constructed a functional association network from the genes we identified as having a differential fitness between the wild-type strain and the polarity mutant based on the interactions available from the STRING database (57–59). The STRING database infers functional associations between proteins by integrating information from several sources, which includes text mining, annotated molecular complexes and computationally predicted interactions. Each interaction is scored based on the quality of the evidence, which allows more weight to be given to high-confidence interactions during downstream processing steps.

Our constructed functional association network could be represented by a largely connected network with only few disconnected nodes (figure 5a). Interestingly, the network showed features of a scale-free structure, suggesting that it can be partitioned into smaller sub-graphs, with genes belonging to one sub-graph are more densely connected to each other than to genes belonging to other sub-graphs. To identify the structure of these sub-graphs, we partitioned the network using a Markov Cluster (MCL) algorithm (60) with the interaction confidence score given by STRING as weights (figure 5b). This procedure revealed 120 clusters, of which 49 consisted of three or more genes. For the seven largest clusters, we performed a gene ontology (GO) enrichment test for biological process GO terms (figure 5b and figure S4). All seven clusters were significantly enriched for one or more GO terms, but no two clusters shared the same GO term enrichment. Five clusters were enriched for terms that can be considered as part of cellular homeostasis: translation, metabolism, signalling, chromatin remodeling and ribosome biogenesis. The other two clusters were enriched for cell polarity and microtubule dynamics, which are both cellular functions required for cell division.

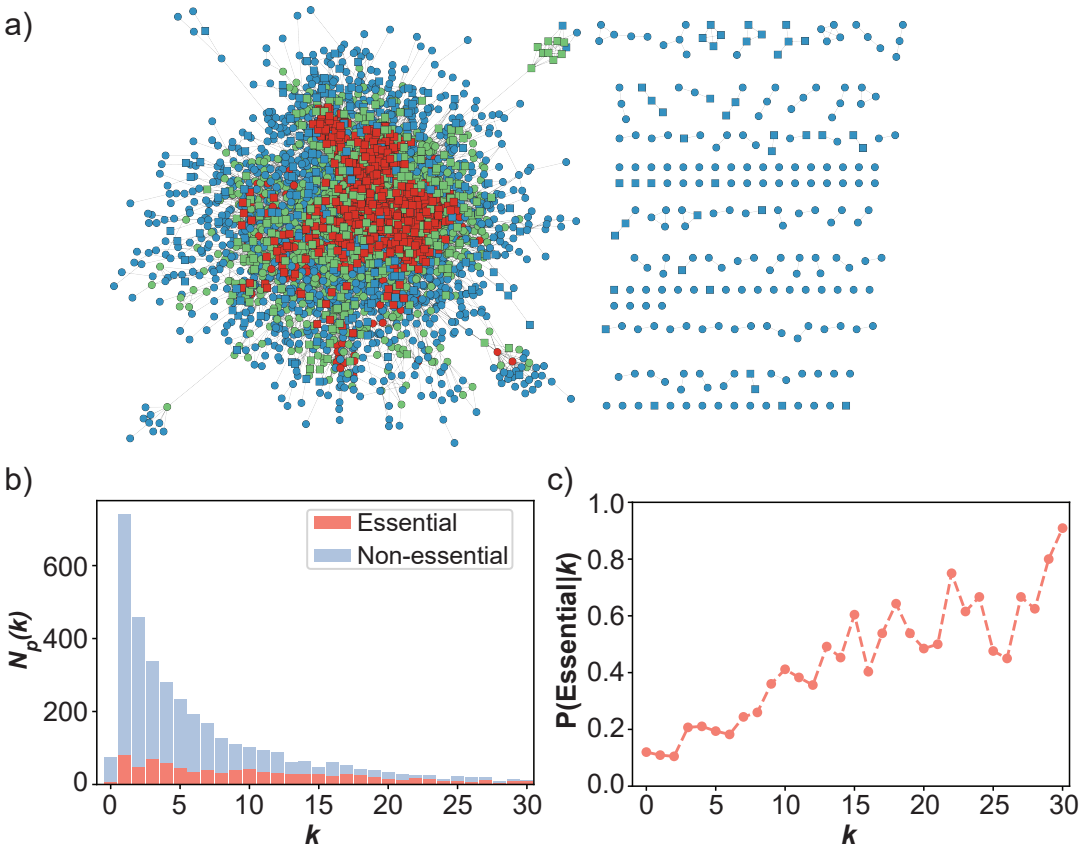

Fig. 3. Gene essentiality correlates with degree in the protein-protein interaction network. (**a**) Visualization of the protein-protein interaction network constructed from the interactions annotated by the BioGRID database. Nodes are colored according to their degree k (blue: $k \leq 3$, green: $4 \leq k \leq 10$, red: $k > 10$). Proteins encoded by essential genes are shown as square nodes, non-essential proteins are shown as circles. (**b**) Stacked histogram of the number of proteins $N_p(k)$ with degree k. Proteins for which the gene is annotated as essential are shown in red, non-essential proteins are shown in blue. The histogram shows that the distribution for k is roughly uniform for essential proteins, while it is skewed towards lower values of k for non-essential proteins. (**c**) The probability that a node is essential as a function of k. The graph displays an increasing trend for the probability as k increases. Combined with the histogram shown in (b), this trend shows that proteins with a high degree are more likely to be essential than proteins with a low degree.

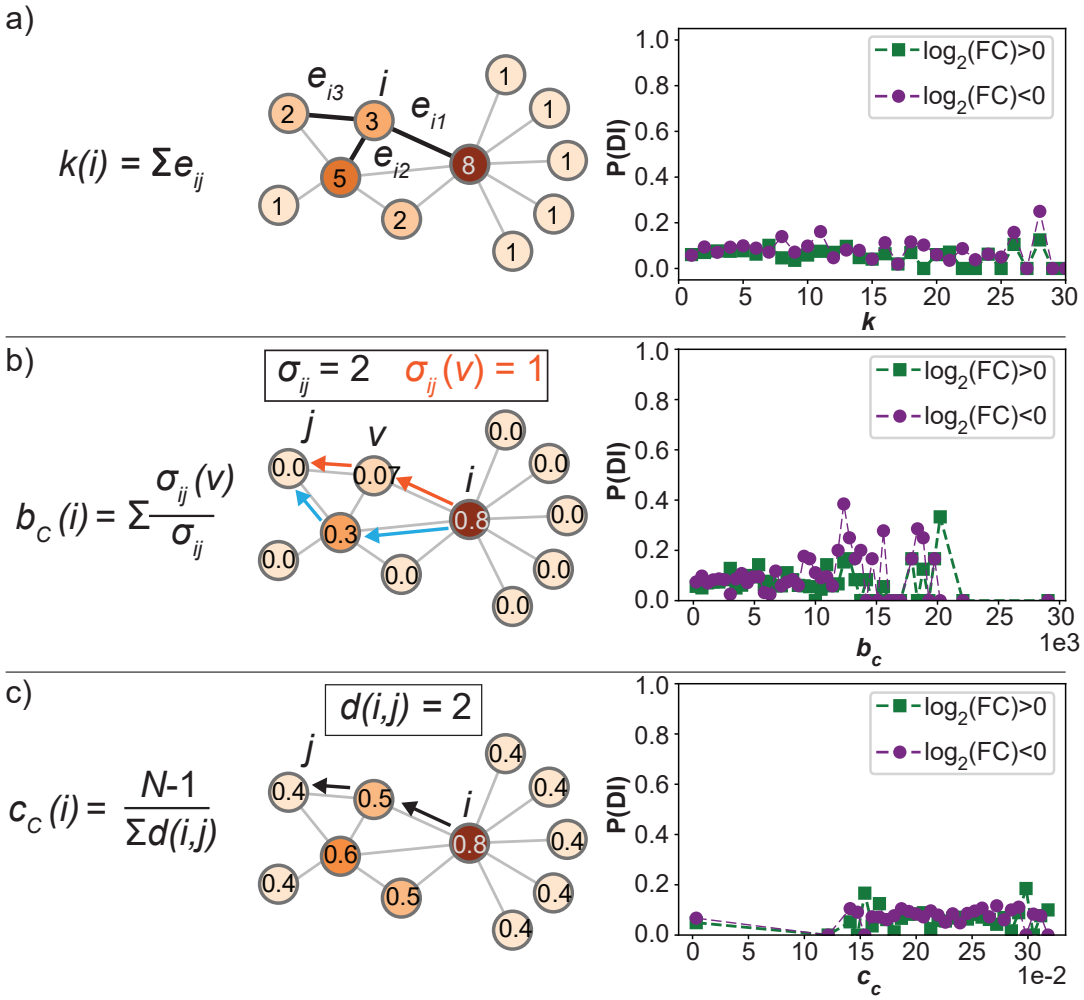

Fig. 4. Changes in gene fitness do not correlate with degree, betweenness and closeness centralities in a protein-protein interaction network. (**a**) The degree centrality k is determined by counting the number of edges e_{ij} a node has connecting it to other nodes in the network. The example graph shows a node i with a degree of three. The plot on the right shows the conditional likelihood P(DI|k) that a node with degree k is a gene with an altered fitness in the polarity mutant. (**b**) The betweenness centrality b_c provides a measure for the importance of a node for the information flow in the network based on the number of shortest paths that pass through that node. In the example there are two shortest paths σ_{ij} from node i to node j, but only one of these paths passes through node v. The plot shows the conditional likelihood P(DI|b_c) that a node with betweenness b_c has an altered disruption tolerance. (**c**) The closeness centrality reflects the distance of a node to all other N nodes in the network based on the average shortest path $d(i,j)$. The example graph shows a node i with a shortest pathlength of two to node j. The plot on the right shows the conditional likelihood P(DI|c_c) that a node with closeness c_c has an altered disruption tolerance. For the three centralities shown in panels (a-c), the distribution of P(DI) is approximately uniform.

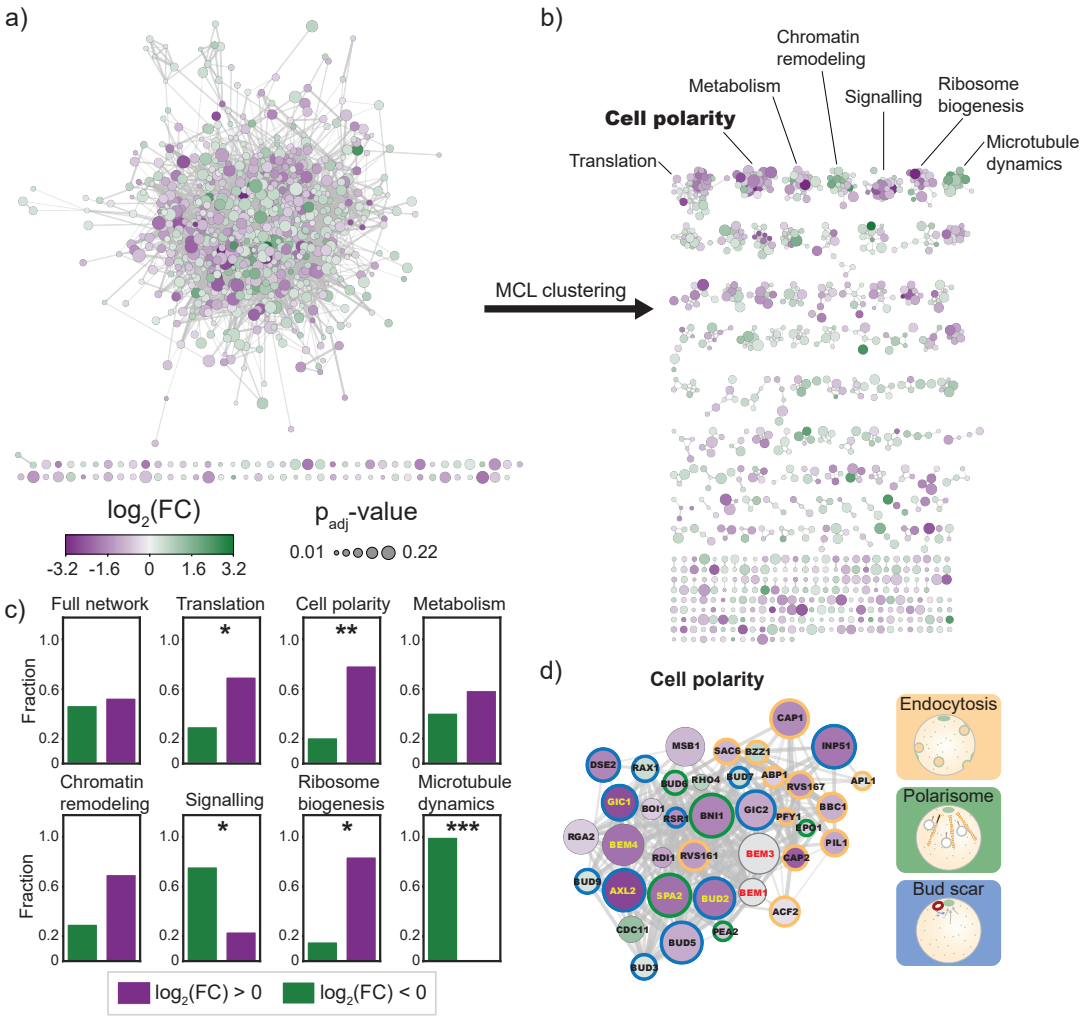

Fig. 5. Clustering of a functional association network reveals diversity of biological processes affected by compensatory evolution (**a**) Graph of the functional association network constructed from genes that have a differential fitness between the wild-type strain and the polarity mutant. Node color scales with the magnitude and sign of the fitness effect, node size scales according to the significance level (adjusted p-value). The graph shows that most genes are contained in a single, densely connected network. (**b**) The clusters formed from the graph shown in (a) by the Markov clustering algorithm (MCL). The clusters are arranged from large (top left) to small (bottom right). The biological process gene ontology enrichment is shown for the seven largest clusters. (**c**) Distribution of genes with a decreased (purple) and increased (green) fitness in the polarity mutant for the seven largest clusters. The clusters enriched for translation, cell polarity, and ribosome biogenesis are enriched for genes with decreased fitness. Conversely, the signalling and microtubule dynamics clusters are enriched for genes with increased fitness. *=$p < 0.05$, **=$p < 0.005$, ***=$p < 5 \cdot 10^{-4}$. The significance level was determined with Fisher's exact test. (**d**) Zoom-in of the cell polarity cluster. The colored rims of the nodes indicate which module of the polarity pathway they belong to. Orange: endocytosis, green: the polarisome, blue: the bud scar.

We also found that the division of genes with increased and decreased fitness deviated significantly from a random partitioning for several clusters (figure 5c). Specifically, the translation and cell polarity clusters were enriched for genes with increased fitness, while the signalling and microtubule dynamics clusters were enriched for genes with decreased fitness. The large number of translation genes with increased fitness could point towards an intolerance to fluctuations in protein copy numbers. Similarly, increased fitness of polarity genes suggests that compensatory evolution causes an increased dependence on modules that act in parallel to the one perturbed. Overall, the increased dispensability of microtubule-related genes was perhaps most surprising, as microtubules perform vital cellular functions such as organelle and spindle positioning (61, 62).

In summary, these results reveal strong functional connections between the genes affected by compensatory evolution. At the same time, a finer partitioning of the genes into sub-graphs shows that they are part of a diverse set of biological processes. Thus, compensatory mutations induce changes that can go beyond the initially perturbed module. Yet, some functional organization does appear to be maintained during evolution, as we find several examples where genes related to the same biological process predominantly share the same directionality of changes in gene fitness.

D. The possible structure of a latent polarity establishment pathway. The large number of genes that we identified as having a differential fitness between the two genetic backgrounds prevents us from directly determining the structure of a latent polarity pathway. However, the presence of a cluster that is enriched for genes related to cell polarity motivated us to analyze this cluster in more detail. In particular, due to their annotation as polarity genes, we considered the genes belonging to this cluster as the most likely candidates to be part of a latent polarity pathway. We annotated the molecular complex or pathway of each gene and found that most could be assigned to one of the following modules: the axial landmark, the polarisome and the endocytosis module (figure 5d). In this section, we use the currently available literature on these proteins to form a hypothesis about how the components of these different modules might interact to reconstitute a pathway for polarity establishment in the absence of Bem1.

D.1. The axial landmark. In wild-type haploid yeast cells, budding occurs next to, but not at, the previous division site. The structure that directs bud formation towards this location is a molecular complex consisting of four proteins (Bud3, Bud4, Axl1 and Axl2) known as the axial landmark (63). These four proteins assemble into a ring-like structure on the membrane during the M phase of the cell cycle, guided by the remnants of the septin ring of the previous budding event. The majority of this ring (Bud3, Bud4 and Axl1) forms only transiently during the M phase and early G1, but a patch of Axl2 remains present on the membrane throughout the cell cycle (64, 65).

Recent work has shown that Cdc42 polarization induced by landmark proteins occurs in two phases of the cell cycle: in early G1 before START (as marked by the nuclear exit of Whi5) and in late G1 after START (66, 67). These two phases of Cdc42 polarization appear to be required for the complete assembly of the components necessary for cell division (66, 68, 69). It has been proposed that distinct positive feedback loops drive Cdc42 polarization towards the axial landmark before and after START (67). Interestingly, the proposed feedback loop acting prior to START does not require Bem1. Instead, the cycling of Cdc42 between an active and inactive state would be mediated by interactions with Rsr1 and Bud3 (70).

Our data shows that the deletion of Axl2 in the polarity mutant has a profoundly more negative effect on fitness than in a wild-type strain (figure 6a), indicating that the communication between this landmark protein and the Cdc42 polarity module plays an important role during bud formation in the polarity mutant. This is further supported by the similar trend for components of the Rsr1-GTPase module (the GAP Bud2, the GEF Bud5 and the GTPase Rsr1), which functionally connects Axl2 to Cdc42 polarity. In addition, we find that the deletion of Gic1 and Gic2 have an increased negative effect on fitness. Gic1 and Gic2 were initially considered to be Cdc42 effectors, but have lately been implied to also play a role upstream of Cdc42 during polarity establishment by reducing the diffusion rate of Cdc42-GTP on the membrane (66, 68), thereby stabilizing the polar cap. It has been proposed that this stabilizing effect of Gic1 and Gic2 relies on their interaction with PIP2 on the plasma membrane (68). Consistent with this, we find that Inp51, which regulates the PIP2 levels, becomes more important when Bem1, Bem3 and Nrp1 are absent.

At first sight, this pattern suggests that pre-START polarization, which is mediated by the GEF activity of Bud3, is capable of promoting post-START polarization and bud emergence in the polarity mutant. This would allow the cells to surpass the requirement of Bem1 activity for efficient polarity establishment. However, if cell polarization in the polarity mutant would rely on the redundancy of the pre- and post-START polarization mechanisms, we would expect to see a strong switch in the essentiality of Bud3 (from non-essential to essential) and Cdc24 (from essential to non-essential). Instead, we find that the tolerance to disruptions in the *BUD3* is even slightly increased, while *CDC24* appears to be essential in both the wild-type strain and the polarity mutant. Thus, the mechanism for polarity establishment in the polarity mutant remains dependent on Cdc24 to act as a GEF for Cdc42.

D.2. The polarisome. The polarisome is a molecular complex that forms at the incipient bud site. It is generally considered to consist of seven components (Spa2, Pea2, Bni1, Bud6, Aip5, Msb3 and Msb4), although the role of Msb3 and Msb4 in the formation of this complex is still unknown (71). Localization of the polarisome during bud formation is dependent on active Cd42 as the Cdc42-effector Gic2 recruits the components Bud6, Bni1 and Spa2 to the incipient bud site (72, 73). At the bud site, Spa2 acts as a scaffold and mediates the assembly of the complex by binding different components of the polarisome (74). Within the polarisome, the proteins Bni1, Bud6 and Aip5 form the nucleation-core that promotes the assembly of F-actin cables towards the bud site (71). Thus, formation of the polarisome is crucial for the directed transport of membrane components towards the bud site and hence for polarized growth.

We find that several core components of the polarisome (Spa2, Bni1, Pea2, Bud6) appear as having a decreased tolerance to disruption of their corresponding gene in our dataset (figure 6b). As the deletion of Bem3 and Nrp1 was originally found to restore the defect in polarity establishment in *bem1*Δ cells (41), we speculate that the increased importance of the polarisome in the polarity mutant is due to a contribution of actin-mediated transport to Cdc42 polarization rather than downstream processes. Thus, while the role of actin-mediated transport has been disputed (75–77), our results suggest that vesicle delivery of active Cdc42 to the polarity cap makes a significant contribution

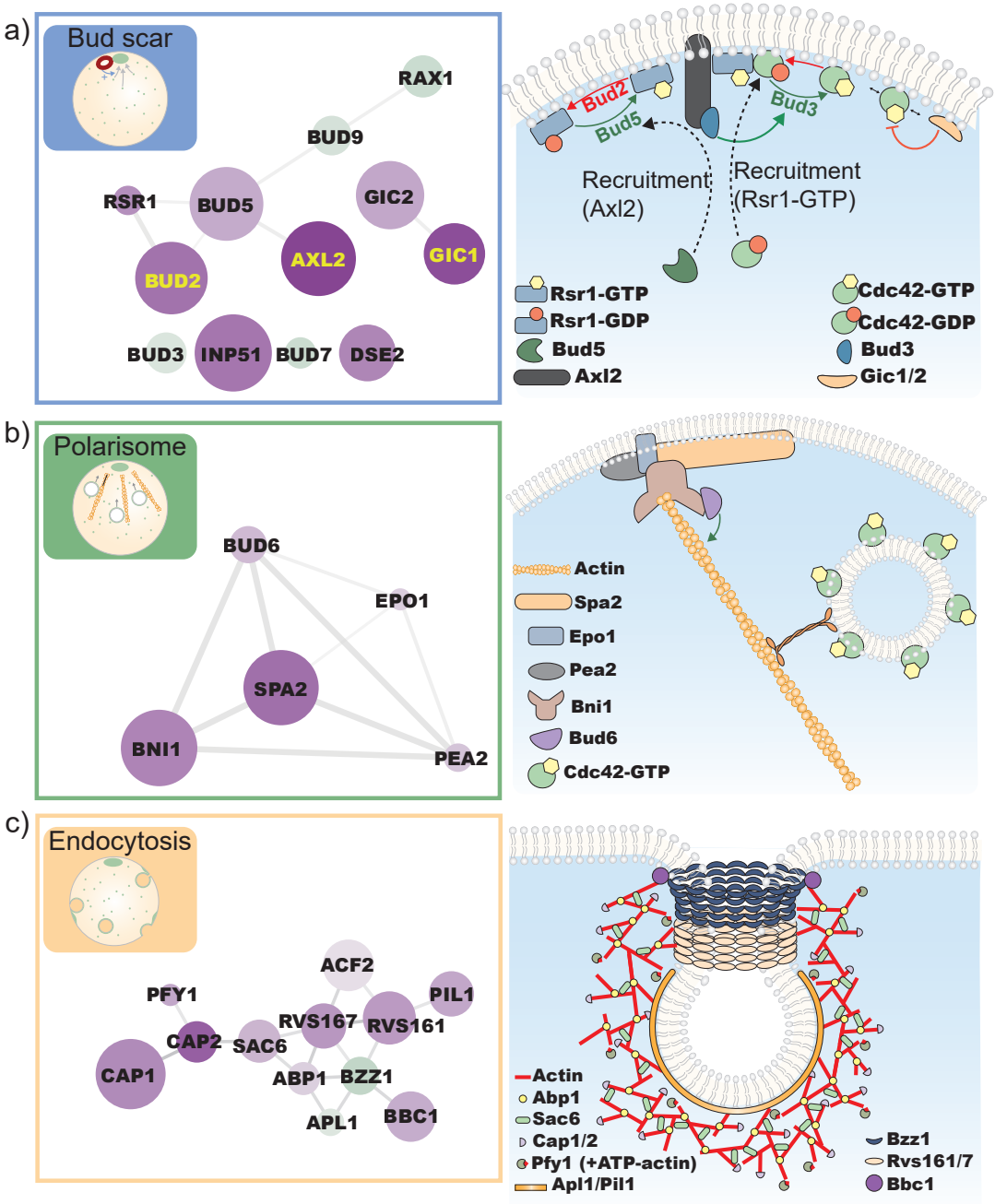

Fig. 6. Processes proposed to mediate the establishment of a latent polarity pathway. As in figure 4, node color scales with the magnitude and sign of the fitness difference, node size scales with the significance value. (**a**) The physical subnetwork of proteins related to the spatial landmark for which the corresponding gene was found to have an altered contribution to fitness between the wild-type strain and polarity mutant. The graph on the left shows that most genes coding for axial landmark proteins (Axl2), proteins of the Rsr1-GTPase module (Bud2, Bud5, Rsr1) and interacting proteins (Gic1, Gic1) become less tolerant to disruption in the polarity mutant. In contrast, components of the bipolar landmark (Rax1, Bud9, Bud7) become more tolerant to disruption. A schematic illustration of the currently proposed mechanism through which the axial landmark can promote Cdc42 polarization is shown on the right. (**b**) Several important components of the polarisome were found to have increased gene fitness in the polarity mutant. The left shows the physical subnetwork of the corresponding polarisome proteins, the right shows a schematic of these physical interactions. Actin cables and myosin have been added to emphasize the role of the polarisome in directing actin-mediated transport towards the polarity spot. (**c**) Genes related to endocytosis that were affected by compensatory evolution were found to have increased fitness in the polarity mutant, with the exception of *BZZ1* and *APL1*. Importantly, all endocytosis genes were involved in actin patch dynamics. The physical subnetwork of the corresponding proteins is shown on the left, an illustration of the location and role of each protein in actin patch formation is given on the right.

to polarity establishment in the absence of Bem1, Bem3 and Nrp1.

D.3. The endocytosis module. Endocytosis occurs through a dense network of short actin cables that generate the force required for invagination of the plasma membrane (78). The formation and dynamics of these actin patches is regulated by the Arp2/3 complex (79, 80). During polarity establishment, active Cdc42 initiates a cascade that recruits and activates the Arp2/3 complex, resulting in the increased formation of actin patches near the site of polarized growth (81). The role of endocytosis in polarity establishment is currently unclear, as it has been proposed to be involved in both positive and negative feedback loops (82–84).

Many of the genes that belong to the cell polarity cluster are related to the regulation of actin, but several proteins stand out as components of actin patches and the endocytic machinery (figure 6c). First of all, we find that the two subunits of the capping protein heterodimer (Cap1 and Cap2) become increasingly important in the polarity mutant. Capping proteins are required for inhibiting the growth of actin filaments to allow the formation of a dense structure of short actin filaments that make up the actin patch (85, 86). Second, we see an increased importance of the BAR-domain containing amphiphysin proteins Rvs161 and Rvs167. These proteins stabilize the curvature of invaginated membranes and promote their scission during endocytosis. The deletion of Rvs161 or Rvs167 has been shown to increase the rate of failure to create endocytic veiscles (2). Lastly, we see the same effect for the adapter protein Abp1 that connects actin patches to the endocytic machinery (87). Taken together, this pattern of increased fitness of genes encoding for proteins involved in actin patch formation and endocytosis indicates that endocytosis makes an important contribution to polarity establishment. Whether this is due to its involvement in a negative or positive feedback loop for Cdc42 polarization remains to be determined.

3. Discussion

In this study, we examined how mutations compensating for a targeted perturbation of a module in the polarity pathway (41) affect the global genotype-fitness relation. To do so, we used a transposon mutagenesis screen to compare the fitness effect of gene disruptions between a wild-type strain and a polarity mutant in which these three genes were deleted. Remarkably, our data shows that the deletion of only three genes changes the fitness of over 10% of the genome. While this percentage is similar to what has been reported by several other studies investigating the background dependency of a mutation's fitness effect (46, 88), these studies typically compare different isolates rather than variants of the same strain. In our case, the two strains are closely related and their genomes should only differ by the three deleted genes. Based on this, we would have expected the set of genes with a differential fitness to be smaller compared to other studies. One possible explanation for the relatively large number of affected genes we find is that our analysis method is focused on discovering changes in gene fitness rather than only changes gene essentiality. Our set therefore contains genes that would likely have remained undetected by other studies. Despite the higher sensitivity of our method, it also has important limitations due to which the number of fitness change reported in this article is likely to be an underestimation. Importantly, because we sum read counts over the entire open reading frame, our analysis is relatively insensitive to domain changes in large genes. Similarly, by only considering coding regions we are unable to identify changes in gene fitness that are related to changes in gene expression levels.

It is possible that the scale at which gene fitness changes occur during compensatory evolution depends on the environment (12, 89). In a recent survey of changes in gene essentiality between natural isolates of *S. cerevisiae*, it was proposed that the majority of the observed variation was due to environmental factors (88). That is, it was argued that most genes that emerged as differentially essential in their screen were caused by strain-specific responses to growth in non-standard media. The mutagenesis screen we performed has a similar limitation. SATAY requires transposition to be induced in media in which galactose is the sole carbon source (45), while the phenotypic similarity between our two strains has only been verified for growth under standard conditions (41). We can therefore not exclude that we would have observed less changes in gene fitness if we had performed a screen in a different environment. However, we expect that the effect of the environment on our results is limited for the following two reasons. First, the overall genetic divergence between our strains should be smaller than what is typical for natural isolates that may have adopted different lifestyles to accommodate to their niche. A different study indeed showed that most genetic interactions are conserved across environments (90). Second, although we did identify a cluster enriched for metabolically related genes in our gene set, genes involved in galactose metabolism or respiration are not overrepresented in this cluster.

With the aim of making a first step towards predictive models, we assessed whether the genes that are affected by compensatory evolution can be identified based on their position in a PPI network (46). Unfortunately, we did not observe any correlation between the likelihood that gene fitness changes and the degree, betweenness and connectedness centralities of the associated proteins. Thus, based on these three centralities, it appears that predictions cannot be made from the structure of the PPI network. While we were able to validate the presence of several features that are typically observed in PPI networks, we cannot reject the possibility that the lack of correlation is a consequence of poor quality of our PPI network. The accuracy of annotated physical interactions is know to substantially vary between datasets (91, 92). To exclude interactions with low confidence, we used the Multi-Validated dataset available from the BioGRID to construct our PPI network. However, network quality does not only depend on the confidence that an interaction exists, but also on the confidence that an interaction is absent (93). In addition, bias is a significant problem in the mapping of interaction networks. Weak and transient interactions are often discarded because they cannot be captured with high confidence by affinity based screens. These interactions could be of particular importance in cases where network structure needs to be recovered in response to gene loss, as recent work identified these interactions as the "glue that holds the cellular network together" (94).

The concept of modularity is, implicitly and explicitly, still strongly embedded in cell and synthetic biology (95, 96). Using the functional associations available from the STRING database, we do indeed find that genes with differential fitness can be clustered, suggesting that some level of modular organization does indeed exist within biological networks. This is further supported by our finding that several clusters are enriched for either genes with increased or decreased fitness. At the same time, our data demonstrates that the compensatory evolution of one module of the polarity pathway affects gene fitness in many other modules, including those that have no clear relation to cell polarization. These findings complement those from an earlier study showing that gene loss can be compensated by mutations in functionally unrelated genes (97), by demonstrating that gene fitness across multiple cellular processes can change during compensatory evolution. It is likely that these changes in gene fitness will affect the further evolution of these modules. Thus, functional modules do not appear to evolve independently of each other, implying that evolvability is not a property that is derived from modularity.

The presence of a cluster enriched for polarity genes suggests that proteins involved in polarity establishment in

the wild-type background may also be involved in the latent pathway for polarity that acts in the absence of Bem1, Bem3 and Nrp1. This finding motivated us to formulate a hypothesis on the possible structure of this latent pathway. Importantly, a more detailed annotation of the genes in this cluster indicates the involvement of endocytosis, the bud scar and the polarisome. While their role in polarity establishment has been an active field of study, we find that the currently known interactions are unable to fully explain the pattern of gene fitness changes we observe in the polarity mutant. For example, a mechanism for Cdc42 polarization that does not depend on Bem1 was previously proposed to drive polarity establishment before START (66, 67, 70). It is therefore tempting to speculate that this mechanism becomes the main driver cell polarization in the polarity mutant. However, the proposition that Bud3 rather than Cdc24 acts as a GEF in this pathway is inconsistent with our finding that the fitness of Bud3 does not increase in the polarity mutant. Instead, the components of the endocytosis, bud scar and polarisome modules may be involved in novel interactions when Bem1, Bem3 and Nrp1 are deleted.

We found that the number of genes that increase fitness and those that decrease fitness after compensatory evolution is nearly equal. Thus, gene loss does not appear to necessarily decrease mutational robustness, but rather cause a restructuring of the gene-fitness relationship. While it is somewhat counterintuitive that gene loss can lead to the increased dispensability of other genes, a mechanistic explanation has been given for this phenomenon. Specifically, if the loss of a protein fully inactivates an associated pathway, the additional loss of other proteins on the same pathway does not incur additional fitness costs (44, 98). In this way, the loss of a protein can appear to buffer mutations in other proteins. However, this explanation does not hold for the case where gene deletions lead to the functional restoration of the perturbed pathway. Similarly, the scale at which we see changes in gene fitness occur and the diversity of cellular processes that are affected suggests an alternative mechanism. How then can the loss of a small number of genes cause changes in the gene-fitness relation of such a large part of the genome? Although our results do not provide direct evidence, we propose that gene loss can induce widespread rewiring of the physical interaction network based on the following reasoning. The fitness effect resulting from the loss of a gene is related to the physiological role of the protein encoded by that gene. However, it is increasingly recognized that a gene does not encode for a protein with a static structure, but rather for structural ensembles (99, 100). Which structure is preferred depends on the environment, making protein function to be heavily context dependent (101). We speculate that in a similar manner, protein structure may be affected on the presence or absence of specific binding partners (102). Loss of one binding partner could in that case cause a conformational change that affects its affinity for other possible binding partners. In this way, the deletion of one protein can initiate a cascade that induces large-scale rewiring of the protein interaction network.

We conclude that modularity plays a minor role during evolution. Compensatory evolution instead appears to induce genome-wide rearrangements in interaction networks which might be mediated by protein promiscuity. Because these genome-wide changes can affect the adaptive potential of many different cellular processes, this could explain how gene loss can promote evolutionary novelty (16, 17, 19, 103–105) and allow populations to escape fitness peaks (17). Despite the minimal role of modularity, some hope for making evolutionary predictions might be drawn from the result that for several instances genes related to the same biological process share the same change in gene fitness after compensatory evolution. Our work also makes a case for the importance of protein ensembles and weak interactions in shaping adaptive pathways. Interactions that are weak in non-perturbed conditions could be driving the re-establishment of biological pathways in response to perturbations. Mapping these weak, non-specific interactions that are frequently perceived as irrelevant will be instrumental to bridge the gap between biological network structure and the evolutionary potential of biological processes.

4. Methods

A. Strains. All strains used in this study are from the W303 genetic background. The cas9 cassette was obtained from plasmid p414-TEF1p-cas9-CYC1t (106) and fused to the up- and downstream genomic sequences of the *HO*-locus and the *ScURA3* marker using overlap-extension PCR. The resulting genetic construct was transformed into the wild-type strain and the polarity mutant using according to a lithium-acetate transformation protocol (107). Correct integration was verified with colony PCR. Endogenous expression of Cas9 from the *HO*-locus had no significant effects on growth. Strains were made compatible with SATAY by removing the *ScURA3* marker and the endogenous *ADE2* locus using the CRISPR/Cas9 system according to the double guide-RNA (gRNA) method of Mans et al. (108). gRNA sequences targeting the *ScURA3* marker and *ADE2* locus were designed using the online toolbox CHOPCHOP (109). The repair fragment for removal of the *ScURA3* marker was constructed by PCR amplification of the genomic sequence upstream and downstream of the *ScURA3* marker and fusing the two fragments using overlap-extension PCR. Similarly, the repair fragment for removal of the *ADE2* locus was constructed by fusing the up- and downstream genomic sequences with overlap-extension PCR. Removal of *ScURA3* marker and the *ADE2* was verified by colony PCR using primers 5 and 6 and primers 7 and 8, respectively. Correct clones were cured from their gRNA plasmids by inoculating them in non-selective medium (YPD) and growing them until saturation (∼1.5 days) at 30 °C. After saturation was reached, the cultures were plated to single colonies on YPD agar plates and screened for the loss of growth on media selecting for the marker of the gRNA plasmid. Strains were stored at -80 °C as frozen stocks in 40% (v/v) glycerol. The double gRNA plasmids that were used as a template were a kind gift from Pascale Daran-Lapujade.

B. Media. Standard culturing and growth assays were performed in YPD (10g/L Yeast extract, 20 g/L Peptone, 20 g/L dextrose), SC (6.9 g/L Yeast nitrogen base, 0.75 g/L Complete supplement mixture, 20 g/L dextrose). For ade^- strains, standard growth media was supplemented with 20 mg/L adenine just before incubation. Liquid media for the preculture and induction steps of SATAY were prepared according to the recipe in table S1. After preparation, the media was filter sterilized using Rapid-Flow Sterile Disposable Filter Units (Nalgene) and stored at 4°C until use. Liquid media for the reseed step of SATAY was prepared by autoclaving 2.6 L of MiliQ water in a 5 L flask. 400 mL of a 7.5X concentrated solution of the nutrients was prepared separately and filter sterilized. To prevent the degradation of media components, this concentrate was stored in the dark at 4°C until used. On the day of reseed, the concentrate was aseptically added to the 5 L flask containing 2.6 L of MiliQ water and mixed. Solid media was prepared by adding 20 g/L agar and 30 mM Tris-HCl (pH 7.0) to the liquid media recipe and autoclaving the mixture for 20 minutes at 121°C. 20 mg/L adenine was aseptically added after autoclaving, unless plates were intended to be selective for adenine auxotrophy.

C. Transposon mutagenesis screens.

C.1. Library generation. SATAY libraries were generated based on the procedure described by (110), which is a modification of the original protocol (111) to allow transposition in liquid media. ade^- cells were transformed with plasmid pBK549 (110), which was a kind gift from Benoît Kornmann, according to a lithium acetate transformation protocol (107). To screen for clones transformed with the intact version of plasmid pBK549 (see (112) for details on the different species of pBK549), 12-24 colonies were picked from the transformation plate, re-streaked on fresh SD-ADE and SD-URA plates and incubated for 3 days at 30°C. For clones that showed full growth on SD-URA plates while producing a small number of colonies on SD-ADE plates, cells were scraped from the SD-URA plate and used to inoculate 25 mL of preculture media at an OD600 of 0.20-0.28. Precultures were grown on an orbital platform shaker at 160 rpm, 30 °C until the OD600 was between 5-7 (∼20h). The saturated precultures were used to inoculate 200 mL of induction media at an OD600 of 0.10-0.27 and grown for 52 hours to allow transposition to occur. The efficiency of transposition was monitored by plating samples of the liquid induction cultures on SD-ADE at T=0 and T=52 hours and scoring the number of colonies on these plates after 3 days of incubation at 30 °C. After 52 hours of induction, the resulting transposon mutagenesis libraries were reseeded in 3 liters of reseed media at an OD600 of 0.21-0.26. Typically, this meant that around 7 million transposon mutants were reseeded per library. Reseeded libraries were grown for 92 hours at 140 rpm, 30 °C. At the end of reseed, cells were harvested by centrifugation of the reseed cultures at 5000 xg for 30 minutes. Cell pellets were stored at -20 °C.

C.2. Genomic DNA extraction. A 500 mg frozen pellet was resuspended in 500 µL cell breaking buffer* and distributed into 280 µL aliquots. 300 µL of 0.4-0.6 mm glass beads (Sigma-Aldrich, G8772) and 200 µL of Phenol:Chloroform:isoamyl alcohol 25:24:1 (Sigma-Aldrich, P2069) were added to each aliquot and cells were lysed by vortexing the samples with

*2% Triton X-100, 1% SDS, 100 mM NaCl, 100 mM Tris-HCl pH8.0, 1 mM EDTA

a Vortex Genie 2 at maximum speed at 4°C for 10 minutes. 200 µL of TE buffer was added to each lysate, after which the samples were centrifuged at 16100x g, 4°C for 5 minutes. After centrifugation, the upper layer (∼400 µL) was transferred to a clean eppendorf tube. 2.5 volumes of 100% absolute ethanol was added to each sample and mixed by inversion to precipitate the genomic DNA. After precipitation, the DNA was pelleted by centrifugation at 16100x g, 20°C for 5 minutes. The supernatant was removed and the DNA pellet was resuspended in 200 µL of 250 µg/ml RNAse A solution (qiagen, Cat. No. 19101). the resuspended DNA pellets were incubated at 55°C for 15 minutes to allow digestion of the RNA. After digestion, 20 µL 3M, pH 5.2 sodium acetate (Merck) and 550 µL 100% absolute ethanol was added to each sample and mix by inversion. DNA was pelleted by centrifugation at 16100x g, 20°C for 5 minutes. Pellets were washed with 70% absolute ethanol and dried at 37°C for 10 minutes or until all ethanol had evaporated. The dried pellets were resuspended in a total volume of 100 µL MiliQ water and the concentration of the genomic DNA samples was quantified on a 0.6% agarose gel using the Eurogentec Smartladder 200bp-10kb as a reference. Prepared DNA samples were stored at -20°C or 4°C until used.

C.3. Library sequencing. To prepare genomic DNA samples for sequencing, 2x2 µg of DNA from each sample were transferred to non-stick microcentrifuge tubes and digested with 50 units of DpnII and NlaIII in a total volume of 50 µL for 17 hours at 37°C. After digestion, the restriction enzymes were heat-inactivated by incubating the samples at 65°C for 20 minutes. Digestion results were qualitatively assessed by visualization on a 1% agarose gel stained with Sybr-Safe. Successfully digested DNA samples were circularized in the same tube using 25 Weiss units of T4 DNA ligase (Thermo Scientific, Catalog #EL0011) at 22°C for 6 hours in a total volume of 400 µL. After ligation, the circularized DNA was precipitated using 1ml 100% absolute ethanol, 20 µL 3M, pH 5.2 sodium acetate (Merck) and 5 µg linear acrylamide (invitrogen, AM9520) as a carrier. DNA was precipitated for at least 2 days at -20°C. Precipitated DNA was pelleted by centrifugation for 20 minutes at 16100x g at 4°C and washed with 1 ml of 70% ethanol. After washing, the DNA was re-pelleted by centrifugation for 20 minutes at 16100x g at 20°C, the supernatant was removed and pellets were dried for 10 minutes a 37°C. Each dried pellet was resuspended in water and used as a template for 20 PCR reactions of 50 µL. Transposon-genome junctions were amplified using the barcoded primers 1 and 2 (table S2) for DpnII digested DNA or primers 3 and 4 (table S2) for NlaIII digested DNA on a thermal cycler (Bio-Rad C1000 Touch). PCR amplified samples were purified using the NucleoSpin Gel and PCR cleanup kit (Macherey-Nagel) and quantified on the NanoDrop 2000 spectrophotometer (Thermo Scientific). For each sample, equal ratios (w/w) of DpnII and NlaIII digested DNA were pooled. Library preparation and sample sequencing were performed by Novogene (UK) Company Limited. Sequencing libraries were prepared with the NEBNext Ultra II DNA Library Prep Kit, omitting the size selection and PCR enrichment steps. DNA libraries were sequenced on the Illumina NovaSeq 6000 platform using Paired-End (PE) sequencing with a read length of 150 bp.

C.4. Sequence alignment. FASTQ files obtained from the NovaSeq 6000 platform were demultiplexed into DpnII and NlaIII digested DNA samples based on the barcodes introduced during PCR amplification. Read pairs with non-matching barcodes were discarded. After demultiplexing, the forward read of each read pair was selected and the sequences upstream of primer 688_minidsSEQ1210 (45) and downstream of the DpnII (GATC) or NlaIII (CATG) restriction site were trimmed. All demultiplexing and trimming steps were performed with BBduk (113) integrated into a home-written pipeline written in Bash. After trimming, the forward reads were aligned to the S288C reference genome (version R64-2-1_20150113) with the Transposonmapper pipeline ((114) version v1.1.4) using the following settings:

- Data type: 'Single-end'
- Trimming software: 'donottrim'
- Alignment settings: '-t 1 -v 2'

D. Volcano plots. Read count distributions were corrected for spikes using the Beta-Geometric correction method and subsequently normalized for differences in transposon density and sequencing depth with the median of ratios normalization (see section A). P-values were generated using the unequal variance independent t-test available from the SciPy library in Python (115) and corrected for multiple hypothesis testing with the Benjamini-Hochberg procedure implemented in the TRANSIT software tool ((116), version 3.2.6). Genes were considered to be essential if they have been annotated as such by the Saccharomyces Genome Database ((117), accessed on 03/17/2006).

E. Physical interaction network analysis. The Multi-Validated (MV) dataset of physical interactions (release BIOGRID-4.4.214) was downloaded from the BioGRID in Tab 3.0 format, which contains all physical interactions that have been validated by at least two different experimental systems or publication sources. The original

set of physical interactions was filtered to obtain only those that correspond to interactions between proteins of *S. cerevisiae*. Interactions inferred from Affinity Capture-RNA or Protein-RNA were excluded from the dataset as these interactions do not represent direct physical interactions between proteins. Network visualizations were made with Cytoscape ((118), version 3.9.1). Network centralities (degree, betweenness and closeness) were calculated using the NetworkX package in Python ((119), version 2.8.4).

F. Functional interaction network analysis. Functional associations between gene products were retrieved from the STRING database (57) through the stringApp plugin ((58), version 1.7.1) of Cytoscape ((118), version 3.9.1). The confidence threshold of the imported interactions from STRING was set to medium (confidence level $\leq$0.40). Markov Clustering (MCL) was performed with the clusterMaker2 (version 2.2) plugin of Cytoscape using the confidence level as edge weight and setting the granularity parameter to 2.5.

5. Acknowledgements

We thank Agnès Michel and Benoît Kornmann for providing the plasmid pBK549 containing the MiniDS transposon system, their help and guidance when setting up the SATAY assays and insightful discussions. We are grateful to Melanie Wijsman and Nicole Bennis for providing us with the plasmids for CRISPR/Cas9 gene editing and their support during troubleshooting. We also thank Leila Iñigo de la Cruz and Gregory van Beek for establishing and maintaining the SATAY data analysis pipeline and their advice regarding data management. L.L. and E.K. gratefully acknowledge funding from the European Research Council under the European Union's Horizon 2020 research and innovation programme (grant agreement 758132).

1. Helen E. Burston, Lymarie Maldonado-Báez, Michael Davey, Benjamen Montpetit, Cayetana Schluter, Beverly Wendland, and Elizabeth Conibear. Regulators of yeast endocytosis identified by systematic quantitative analysis. *Journal of Cell Biology*, 185(6):1097–1110, 6 2009. ISSN 1540-8140. . URL https://rupress.org/jcb/article/185/6/1097/35216/Regulators-of-yeast-endocytosis-identified-by.
2. Marko Kaksonen, Christopher P. Toret, and David G. Drubin. A Modular Design for the Clathrin- and Actin-Mediated Endocytosis Machinery. *Cell*, 123(2):305–320, 10 2005. ISSN 00928674. . URL https://linkinghub.elsevier.com/retrieve/pii/S0092867405009785.
3. Thomas D. Pollard and Ben O'Shaughnessy. Molecular Mechanism of Cytokinesis. *Annual Review of Biochemistry*, 88(1):661–689, 6 2019. ISSN 0066-4154. . URL https://www.annualreviews.org/doi/10.1146/annurev-biochem-062917-012530.
4. Wouter-Jan Jan Rappel and Leah Edelstein-Keshet. Mechanisms of cell polarization. *Current Opinion in Systems Biology*, 3:43–53, 6 2017. ISSN 24523100. . URL https://linkinghub.elsevier.com/retrieve/pii/S2452310016300166.
5. Elizabeth Conibear. Converging views of endocytosis in yeast and mammals. *Current Opinion in Cell Biology*, 22(4):513–518, 8 2010. ISSN 09550674. . URL https://linkinghub.elsevier.com/retrieve/pii/S0955067410000724.
6. Eveline T Diepeveen, Thies Gehrmann, Valérie Pourquié, Thomas Abeel, and Liedewij Laan. Patterns of Conservation and Diversification in the Fungal Polarization Network. *Genome Biology and Evolution*, 10(7):1765–1782, 7 2018. ISSN 1759-6653. . URL https://academic.oup.com/gbe/article/10/7/1765/5040802.
7. Mohan K. Balasubramanian, Erfei Bi, and Michael Glotzer. Comparative Analysis of Cytokinesis in Budding Yeast, Fission Yeast and Animal Cells. *Current Biology*, 14(18):R806–R818, 9 2004. ISSN 09609822. . URL https://linkinghub.elsevier.com/retrieve/pii/S0960982204006980.
8. Jolien JE van Hooff, Eelco Tromer, Leny M van Wijk, Berend Snel, and Geert JPL Kops. Evolutionary dynamics of the kinetochore network in eukaryotes as revealed by comparative genomics. *EMBO reports*, 18(9):1559–1571, 9 2017. ISSN 1469-221X. . URL https://www.embopress.org/doi/10.15252/embr.201744102.
9. Vagheesh M Narasimhan, Karen A Hunt, Dan Mason, Christopher L Baker, Konrad J Karczewski, Michael R Barnes, Anthony H Barnett, Chris Bates, Srikanth Bellary, Nicholas A Bockett, Kristina Giorda, Christopher J Griffiths, Harry Hemingway, Zhilong Jia, M Ann Kelly, Hajrah A Khawaja, Monkol Lek, Shane McCarthy, Rosie McEachan, Anne O'Donnell-Luria, Kenneth Paigen, Constantinos A Parisinos, Eamonn Sheridan, Laura Southgate, Louise Tee, Mark Thomas, Yali Xue, Michael Schnall-Levin, Petko M Petkov, Chris Tyler-Smith, Eamonn R Maher, Richard C Trembath, Daniel G MacArthur, John Wright, Richard Durbin, and David A van Heel. Health and population effects of rare gene knockouts in adult humans with related parents. *Science*, 352(6284):474–477, 4 2016. . URL https://doi.org/10.1126/science.aac8624.
10. Thomas LaBar, Yu-Ying Phoebe Hsieh, Marco Fumasoni, and Andrew W. Murray. Evolutionary Repair Experiments as a Window to the Molecular Diversity of Life. *Current Biology*, 30(10):R565–R574, 5 2020. ISSN 09609822. . URL https://linkinghub.elsevier.com/retrieve/pii/S0960982220304164.
11. Béla Szamecz, Gábor Boross, Dorottya Kalapis, Károly Kovács, Gergely Fekete, Zoltán Farkas, Viktória Lázár, Mónika Hrtyan, Patrick Kemmeren, Marian J. A. Groot Koerkamp, Edit Rutkai, Frank C. P. Holstege, Balázs Papp, and Csaba Pál. The Genomic Landscape of Compensatory Evolution. *PLoS Biology*, 12(8):e1001935, 8 2014. ISSN 1545-7885. . URL https://dx.plos.org/10.1371/journal.pbio.1001935www.plosbiology.orghttp://www.ncbi.nlm.nih.gov/pubmed/25157590.
12. Marie Filteau, Véronique Hamel, Marie-Christine Pouliot, Isabelle Gagnon-Arsenault, Alexandre K Dubé, and Christian R Landry. Evolutionary rescue by compensatory mutations is constrained by genomic and environmental backgrounds. *Molecular Systems Biology*, 11(10):832, 2015. ISSN 1744-4292. .
13. Farah Kobaisi, Nour Fayyad, Eric Sulpice, Bassam Badran, Hussein Fayyad-Kazan, Walid Rachidi, and Xavier Gidrol. High-throughput synthetic rescue for exhaustive characterization of suppressor mutations in human genes. *Cellular and Molecular Life Sciences*, 77(21):4209–4222, 11 2020. ISSN 1420-682X. . URL http://link.springer.com/10.1007/s00018-020-03519-6.
14. Jacob L. Steenwyk, Dana A. Opulente, Jacek Kominek, Xing-Xing Shen, Xiaofan Zhou, Abigail L. Labella, Noah P. Bradley, Brandt F. Eichman, Neža Čadež, Diego Libkind, Jeremy DeVirgilio, Amanda Beth Hulfachor, Cletus P. Kurtzman, Chris Todd Hittinger, and Antonis Rokas. Extensive loss of cell-cycle and DNA repair genes in an ancient lineage of bipolar budding yeasts. *PLOS Biology*, 17(5):e3000255, 5 2019. ISSN 1545-7885. . URL https://dx.plos.org/10.1371/journal.pbio.3000255.
15. Geert J.P.L. Kops, Berend Snel, and Eelco C. Tromer. Evolutionary Dynamics of the Spindle Assembly Checkpoint in Eukaryotes. *Current Biology*, 30(10):R589–R602, 5 2020. ISSN 09609822. . URL https://linkinghub.elsevier.com/retrieve/pii/S0960982220301949.
16. Zoltán Farkas, Károly Kovács, Zsuzsa Sarkadi, Dorottya Kalapis, Gergely Fekete, Fanni Birtyik, Ferhan Ayaydin, Csaba Molnár, Péter Horváth, Csaba Pál, and Balázs Papp. Gene loss and compensatory evolution promotes the emergence of morphological novelties in budding yeast. *Nature Ecology & Evolution*, 6(6):763–773, 4 2022. ISSN 2397-334X. . URL https://www.nature.com/articles/s41559-022-01730-1.
17. Jana Helsen, Karin Voordeckers, Laura Vanderwaeren, Toon Santermans, Maria Tsontaki, Kevin J Verstrepen, and Rob Jelier. Gene Loss Predictably Drives Evolutionary Adaptation. *Molecular Biology and Evolution*, 37(10):2989–3002, 2020. ISSN 0737-4038. . URL https://academic.oup.com/mbe/article/37/10/2989/5870834.
18. Etienne Rajon and Joanna Masel. Compensatory Evolution and the Origins of Innovations. *Genetics*, 193(4):1209–1220, 4 2013. ISSN 00166731. . URL https://academic.oup.com/genetics/article/193/4/1209/5935314.
19. Alison K Hottes, Peter L Freddolino, Anupama Khare, Zachary N Donnell, Julia C Liu, and Saeed Tavazoie. Bacterial Adaptation through Loss of Function. *PLoS Genetics*, 9(7):e1003617, 7 2013. ISSN 1553-7404. . URL https://www.ncbi.nlm.nih.gov/pubmed/23874220https://dx.plos.org/10.1371/journal.pgen.1003617.
20. Leland H Hartwell, John J Hopfield, Stanislas Leibler, and Andrew W Murray. From molecular to modular cell biology. *Nature*, 402(S6761):C47–C52, 12 1999. ISSN 0028-0836. . URL https://www.nature.com/articles/35011540http://www.nature.com/articles/35011540.
21. Dirk M. Lorenz, Alice Jeng, and Michael W. Deem. The emergence of modularity in biological systems. *Physics of Life Reviews*, 8(2):129–160, 6 2011. ISSN 15710645. . URL www.elsevier.com/locate/plrev.
22. Paul B Rainey and Tim F Cooper. Evolution of bacterial diversity and the origins of modularity. *Research in Microbiology*, 155(5):370–375, 6 2004. ISSN 09232508. . URL https://linkinghub.elsevier.com/retrieve/pii/S0923250804000622.
23. Günter P. Wagner, Mihaela Pavlicev, and James M. Cheverud. The road to modularity. *Nature Reviews Genetics*, 8(12):921–931, 12 2007. ISSN 1471-0056. . URL https://www.nature.com/articles/nrg2267.
24. R Mahadevan and D R Lovley. The Degree of Redundancy in Metabolic Genes Is Linked to Mode of Metabolism. *Biophysical Journal*, 94(4):1216–1220, 2 2008. ISSN 0006-3495. . URL http://www.cell.com/article/S0006349508706398/fulltexthttp://www.cell.com/article/S0006349508706398/abstracthttps://www.cell.com/biophysj/abstract/S0006-3495(08)70639-8.
25. Peter Bieling, Liedewij Laan, Henry Schek, E. Laura Munteanu, Linda Sandblad, Marileen Dogterom, Damian Brunner, and Thomas Surrey. Reconstitution of a microtubule plus-end tracking system in vitro. *Nature*, 450(7172):1100–1105, 12 2007. ISSN 0028-0836. . URL https://www.nature.com/articles/nature06386.
26. Anthony G. Vecchiarelli, Min Li, Michiyo Mizuuchi, and Kiyoshi Mizuuchi. Differential affinities of <scp>MinD</scp> and <scp>MinE</scp> to anionic phospholipid influence <scp>Min</scp> patterning dynamics in vitro. *Molecular Microbiology*, 93(3):453–463, 8 2014. ISSN 0950-382X. . URL https://onlinelibrary.wiley.com/doi/10.1111/mmi.12669.
27. Neta Agmon, Jasmine Temple, Zuojian Tang, Tobias Schraink, Maayan Baron, Jun Chen, Paolo Mita, James A Martin, Benjamin P Tu, Itai Yanai, David Fenyõ, and Jef D Boeke. Phylogenetic debugging of a complete human biosynthetic pathway transplanted into yeast. *Nucleic Acids Research*, 11 2019. ISSN 0305-1048. . URL https://academic.oup.com/nar/advance-article/doi/10.1093/nar/gkz1098/5634032.
28. Niels G. A. Kuijpers, Daniel Solis-Escalante, Marijke A. H. Luttik, Markus M. M. Bisschops, Francine J. Boonekamp, Marcel van den Broek, Jack T. Pronk, Jean-Marc Daran, and Pascale Daran-Lapujade. Pathway swapping: Toward modular engineering of essential cellular processes. *Proceedings of the National Academy of Sciences*, 113(52):15060–15065, 12 2016. ISSN 0027-8424. . URL https://pnas.org/doi/full/10.1073/pnas.1606701113.
29. H. Hsu, E. Huang, X.C. Yang, A. Karschin, C. Labarca, A. Figl, B. Ho, N. Davidson, and H.A. Lester. Slow and incomplete inactivations of voltage-gated channels dominate encoding in synthetic neurons. *Biophysical Journal*, 65(3):1196–1206, 9 1993. ISSN 00063495. . URL https://linkinghub.elsevier.com/retrieve/pii/S0006349593811536.
30. Marc Kirschner and John Gerhart. Evolvability. *Proceedings of the National Academy of Sciences*, 95(15):8420–8427, 7 1998. ISSN 0027-8424. . URL https://pnas.org/doi/full/10.1073/pnas.95.15.8420.
31. Thomas F Hansen. Is modularity necessary for evolvability?: Remarks on the relationship between pleiotropy and evolvability. *Biosystems*, 69(2-3):83–94, 2003. ISSN 0303-2647. .
32. Nadav Kashtan, Avi E. Mayo, Tomer Kalisky, and Uri Alon. An Analytically Solvable Model for Rapid Evolution of Modular Structure. *PLoS Computational Biology*, 5(4):e1000355, 4 2009. ISSN 1553-7358. . URL https://dx.plos.org/10.1371/journal.pcbi.1000355.
33. Kirsten H. ten Tusscher and Paulien Hogeweg. Evolution of Networks for Body Plan Patterning; Interplay of Modularity, Robustness and Evolvability. *PLoS Computational Biology*, 7(10):e1002208, 10 2011. ISSN 1553-7358. . URL https://dx.plos.org/10.1371/journal.pcbi.1002208.
34. Berend Snel and Martijn A. Huynen. Quantifying Modularity in the Evolution of Biomolecular Systems. *Genome Research*, 14(3):391–397, 3 2004. ISSN 1088-9051. . URL http://genome.cshlp.org/lookup/doi/10.1101/gr.1969504.
35. Sandrine Etienne-Manneville. Cdc42 - the centre of polarity. *Journal of Cell Science*, 117(8):1291–1300, 2004. ISSN 0021-9533. . URL https://journals.biologists.com/jcs/article/117/8/1291/28257/Cdc42-the-centre-of-polarity.
36. Barry J Thompson. Cell polarity: models and mechanisms from yeast, worms and flies. *Development*, 140(1):13–21, 1 2013. ISSN 0950-1991. . URL https://journals.biologists.com/dev/article/140/1/13/76512/Cell-polarity-models-and-mechanisms-from-yeast.
37. Philipp Glock, Fridtjof Brauns, Jacob Halatek, Erwin Frey, and Petra Schwille. Design of biochemical pattern forming systems from minimal motifs. *eLife*, 8, 11 2019. ISSN 2050-084X. . URL https://elifesciences.org/articles/48646.
38. Vassili Ivanov and Kiyoshi Mizuuchi. Multiple modes of interconverting dynamic pattern formation by bacterial cell division proteins. *Proceedings of the National Academy of Sciences*, 107(18):8071–8078, 5 2010. ISSN 0027-8424. . URL https://pnas.org/doi/full/10.1073/pnas.0911036107.
39. Yaron Caspi and Cees Dekker. Mapping out Min protein patterns in fully confined fluidic chambers. *eLife*, 5, 11 2016. ISSN 2050-084X. . URL https://elifesciences.org/articles/19271.

40. Kim J. A. Vendel, Sophie Tschirpke, Fayezeh Shamsi, Marileen Dogterom, and Liedewij Laan. Minimal in vitro systems shed light on cell polarity. *Journal of Cell Science*, 132(4), 2 2019. ISSN 1477-9137. . URL https://journals.biologists.com/jcs/article/132/4/jcs217554/57490/Minimal-in-vitro-systems-shed-light-on-cell.
41. Liedewij Laan, John H Koschwanez, and Andrew W Murray. Evolutionary adaptation after crippling cell polarization follows reproducible trajectories. *eLife*, 4, 2015. .
42. Ben Klünder, Tina Freisinger, Roland Wedlich-Söldner, and Erwin Frey. GDI-Mediated Cell Polarization in Yeast Provides Precise Spatial and Temporal Control of Cdc42 Signaling. *PLOS Computational Biology*, 9(12):e1003396, 12 2013. ISSN 1553-7358. . URL https://journals.plos.org/ploscompbiol/article?id=10.1371/journal.pcbi.1003396.
43. Fridtjof Brauns, Leila Iñigo de la Cruz, Werner K.-G. Daalman, Ilse de Bruin, Jacob Halatek, Liedewij Laan, and Erwin Frey. Redundancy and the role of protein copy numbers in the cell polarization machinery of budding yeast. *Nature Communications*, 14(1):6504, 10 2023. ISSN 2041-1723. . URL https://www.nature.com/articles/s41467-023-42100-0.
44. Jolanda van Leeuwen, Carles Pons, Charles Boone, and Brenda J. Andrews. Mechanisms of suppression: The wiring of genetic resilience. *BioEssays*, 39(7), 7 2017. ISSN 0265-9247. . URL https://onlinelibrary.wiley.com/doi/10.1002/bies.201700042.
45. Agnès H. Michel, Riko Hatakeyama, Philipp Kimmig, Meret Arter, Matthias Peter, Joao Matos, Claudio De Virgilio, and Benoît Kornmann. Functional mapping of yeast genomes by saturated transposition. *eLife*, 6, 5 2017. ISSN 2050-084X. . URL https://elifesciences.org/articles/23570.
46. Marco Galardini, Bede P Busby, Cristina Vieitez, Alistair S Dunham, Athanasios Typas, and Pedro Beltrao. The impact of the genetic background on gene deletion phenotypes in Saccharomyces cerevisiae. *Molecular Systems Biology*, 15(12):e8831, 12 2019. ISSN 1744-4292. . URL /pmc/articles/PMC6901017//pmc/articles/PMC6901017/?report=abstracthttps://www.ncbi.nlm.nih.gov/pmc/articles/PMC6901017/https://onlinelibrary.wiley.com/doi/full/10.15252/msb.20198831https://onlinelibrary.wiley.com/doi/abs/10.15252/msb.20198831https://.
47. Maliackal Poulo Joy, Amy Brock, Donald E Ingber, and Sui Huang. High-Betweenness Proteins in the Yeast Protein Interaction Network. *BioMed Research International*, 2005(2):96–103, 6 2005. ISSN 2314-6133. . URL https://www.hindawi.com/journals/bmri/2005/594674/.
48. Hunter B. Fraser, Aaron E. Hirsh, Lars M. Steinmetz, Curt Scharfe, and Marcus W. Feldman. Evolutionary Rate in the Protein Interaction Network. *Science*, 296(5568):750–752, 4 2002. ISSN 0036-8075. . URL https://www.science.org/doi/10.1126/science.1068696http://www.ncbi.nlm.nih.gov/pubmed/11976460.
49. Elena Zotenko, Julian Mestre, Dianne P O'Leary, and Teresa M Przytycka. Why Do Hubs in the Yeast Protein Interaction Network Tend To Be Essential: Reexamining the Connection between the Network Topology and Essentiality. *PLoS Computational Biology*, 4(8), 8 2008. ISSN 1553734X. . URL /pmc/articles/PMC2467474//pmc/articles/PMC2467474/?report=abstracthttps://www.ncbi.nlm.nih.gov/pmc/articles/PMC2467474/.
50. H Jeong, S P Mason, A.-L. Barabási, and Z N Oltvai. Lethality and centrality in protein networks. *Nature*, 411(6833):41–42, 2001. ISSN 0028-0836. . URL https://www.nature.com/articles/35075138http://www.nature.com/articles/35075138.
51. C. Stark. BioGRID: a general repository for interaction datasets. *Nucleic Acids Research*, 34(90001):D535–D539, 1 2006. ISSN 0305-1048. . URL https://academic.oup.com/nar/article-lookup/doi/10.1093/nar/gkj109.
52. Rose Oughtred, Jennifer Rust, Christie Chang, Bobby-Joe Breitkreutz, Chris Stark, Andrew Willems, Lorrie Boucher, Genie Leung, Nadine Kolas, Frederick Zhang, Sonam Dolma, Jasmin Coulombe-Huntington, Andrew Chatr-aryamontri, Kara Dolinski, and Mike Tyers. The <scp>BioGRID</scp> database: A comprehensive biomedical resource of curated protein, genetic, and chemical interactions. *Protein Science*, 30(1):187–200, 1 2021. ISSN 0961-8368. . URL https://onlinelibrary.wiley.com/doi/10.1002/pro.3978.
53. Mikaela Koutrouli, Evangelos Karatzas, David Paez-Espino, and Georgios A Pavlopoulos. A Guide to Conquer the Biological Network Era Using Graph Theory. *Frontiers in Bioengineering and Biotechnology*, 8:34, 1 2020. ISSN 2296-4185. . URL http://www.ncbi.nlm.nih.gov/pubmed/32083072http://www.pubmedcentral.nih.gov/articlerender.fcgi?artid=PMC7004966https://www.frontiersin.org/article/10.3389/fbioe.2020.00034/full.
54. André C. Michaelis, Andreas-David Brunner, Maximilian Zwiebel, Florian Meier, Maximilian T. Strauss, Isabell Bludau, and Matthias Mann. The social and structural architecture of the yeast protein interactome. *Nature*, 624(7990):192–200, 12 2023. ISSN 0028-0836. . URL https://www.nature.com/articles/s41586-023-06739-5.
55. Michael P H Stumpf, Piers J Ingram, Ian Nouvel, and Carsten Wiuf. Statistical Model Selection Methods Applied to Biological Networks. In Corrado Priami, Emanuela Merelli, Pablo Gonzalez, and Andrea Omicini, editors, *Transactions on Computational Systems Biology III*, pages 65–77. Springer Berlin Heidelberg, Berlin, Heidelberg, 2005. ISBN 978-3-540-31446-2. . URL http://link.springer.com/10.1007/11599128_5.
56. Ziyun Ding and Daisuke Kihara. Computational identification of protein-protein interactions in model plant proteomes. *Scientific Reports*, 9(1):8740, 6 2019. ISSN 2045-2322. . URL https://www.nature.com/articles/s41598-019-45072-8.
57. Damian Szklarczyk, Annika L Gable, Katerina C Nastou, David Lyon, Rebecca Kirsch, Sampo Pyysalo, Nadezhda T Doncheva, Marc Legeay, Tao Fang, Peer Bork, Lars J Jensen, and Christian von Mering. The STRING database in 2021: customizable protein–protein networks, and functional characterization of user-uploaded gene/measurement sets. *Nucleic Acids Research*, 49(D1):D605–D612, 1 2021. ISSN 0305-1048. . URL https://academic.oup.com/nar/article/49/D1/D605/6006194.
58. Nadezhda T Doncheva, John H Morris, Jan Gorodkin, and Lars J Jensen. Cytoscape StringApp: Network Analysis and Visualization of Proteomics Data. *Journal of Proteome Research*, 18(2):623–632, 2 2019. ISSN 1535-3893. . URL https://pubs.acs.org/doi/full/10.1021/acs.jproteome.8b00702http://www.ncbi.nlm.nih.gov/pubmed/30450911http://www.pubmedcentral.nih.gov/articlerender.fcgi?artid=PMC6800166https://pubs.acs.org/doi/10.1021/acs.jproteome.8b00702.
59. Damian Szklarczyk, Annika L. Gable, David Lyon, Alexander Junge, Stefan Wyder, Jaime Huerta-Cepas, Milan Simonovic, Nadezhda T. Doncheva, John H. Morris, Peer Bork, Lars J. Jensen, and Christian von Mering. STRING v11: protein–protein association networks with increased coverage, supporting functional discovery in genome-wide experimental datasets. *Nucleic Acids Research*, 47(D1):D607–D613, 1 2019. ISSN 0305-1048. . URL https://pubmed.ncbi.nlm.nih.gov/30476243/https://academic.oup.com/nar/article/47/D1/D607/5198476http://www.ncbi.nlm.nih.gov/pubmed/30476243http://www.pubmedcentral.nih.gov/articlerender.fcgi?artid=PMC6323986.
60. Stijn Van Dongen. Graph Clustering Via a Discrete Uncoupling Process. *SIAM Journal on Matrix Analysis and Applications*, 30(1):121–141, 1 2008. ISSN 0895-4798. . URL https://doi.org/10.1137/040608635http://epubs.siam.org/doi/10.1137/040608635.
61. Janet L. Carminati and Tim Stearns. Microtubules Orient the Mitotic Spindle in Yeast through Dynein-dependent Interactions with the Cell Cortex. *The Journal of Cell Biology*, 138(3):629, 8 1997. ISSN 00219525. . URL /pmc/articles/PMC2141630//pmc/articles/PMC2141630/?report=abstracthttps://www.ncbi.nlm.nih.gov/pmc/articles/PMC2141630/.
62. Istvan R. Boldogh, Hyeong-Cheol Yang, and Liza A. Pon. Mitochondrial Inheritance in Budding Yeast. *Traffic*, 2(6):368–374, 6 2001. ISSN 1398-9219. . URL https://onlinelibrary.wiley.com/doi/10.1034/j.1600-0854.2001.002006368.x.
63. John Chant. Control of cell polarity by internal programs and external signals in yeast. *Seminars in Developmental Biology*, 6(1):13–23, 2 1995. ISSN 10445781. . URL https://linkinghub.elsevier.com/retrieve/pii/S1044578106800812.
64. Xiang-Dong Gao, Lauren M Sperber, Steven A Kane, Zongtian Tong, Amy Hin Yan Tong, Charles Boone, and Erfei Bi. Sequential and Distinct Roles of the Cadherin Domain-containing Protein Axl2p in Cell Polarization in Yeast Cell Cycle. *Molecular Biology of the Cell*, 18(7):2542–2560, 7 2007. ISSN 1059-1524. . URL https://www.molbiolcell.org/doi/10.1091/mbc.e06-09-0822.
65. Pil Jung Kang, Elizabeth Angerman, Chan-Hun Jung, and Hay-Oak Park. Bud4 mediates the cell-type-specific assembly of the axial landmark in budding yeast. *Journal of Cell Science*, 125(16):3840–3849, 1 2012. ISSN 1477-9137. . URL https://journals.biologists.com/jcs/article/125/16/3840/32525/Bud4-mediates-the-cell-type-specific-assembly-ofhttps://journals.biologists.com/jcs/article/doi/10.1242/jcs.103697/263119/Bud4-mediates-the-cell-type-specific-assembly-of.
66. Kristi E Miller, Pil Jung Kang, and Hay Oak Park. Regulation of Cdc42 for polarized growth in budding yeast. *Microbial Cell*, 7(7):175, 7 2020. ISSN 23112638. .
67. Kyle D Moran, Hui Kang, Ana V Araujo, Trevin R Zyla, Koji Saito, Denis Tsygankov, and Daniel J Lew. Cell-cycle control of cell polarity in yeast. *Journal of Cell Biology*, 218(1):171–189, 1 2019. ISSN 0021-9525. . URL https://doi.org/10.1083/jcb.201806196.
68. Pil Jung Kang, Kristi E Miller, Julia Guegueniat, Laure Beven, and Hay-Oak Park. The shared role of the Rsr1 GTPase and Gic1/Gic2 in Cdc42 polarization. *Molecular Biology of the Cell*, 29(20):2359–2369, 8 2018. ISSN 1059-1524. .
69. Helen Lai, Jian-Geng Chiou, Anastasia Zhurikhina, Trevin R Zyla, Denis Tsygankov, and Daniel J Lew. Temporal regulation of morphogenetic events in Saccharomyces cerevisiae. *Molecular Biology of the Cell*, 29(17):2069–2083, 8 2018. ISSN 1059-1524. . URL https://www.molbiolcell.org/doi/10.1091/mbc.E18-03-0188http://www.ncbi.nlm.nih.gov/pubmed/29927361http://www.pubmedcentral.nih.gov/articlerender.fcgi?artid=PMC6232962.
70. Pil Jung Kang, Mid Eum Lee, and Hay-Oak Park. Bud3 activates Cdc42 to establish a proper growth site in budding yeast. *Journal of Cell Biology*, 206(1):19–28, 7 2014. ISSN 1540-8140. . URL www.jcb.org/cgi/doi/10.1083/jcb.201402040http://www.ncbi.nlm.nih.gov/pubmed/25002677http://www.pubmedcentral.nih.gov/articlerender.fcgi?artid=PMC4085707https://rupress.org/jcb/article/206/1/19/37593/Bud3-activates-Cdc42-to-establish-a-proper-growth.
71. Ying Xie and Yansong Miao. Polarisome assembly mediates actin remodeling during polarized yeast and fungal growth. *Journal of Cell Science*, 134(1), 1 2021. ISSN 14779137. . URL https://journals.biologists.com/jcs/article/134/1/jcs247916/237100/Polarisome-assembly-mediates-actin-remodeling.
72. Hsin Chen, Chun-Chen Kuo, Hui Kang, Audrey S Howell, Trevin R Zyla, Michelle Jin, and Daniel J Lew. Cdc42p regulation of the yeast formin Bni1p mediated by the effector Gic2p. *Molecular biology of the cell*, 23(19):3814–3826, 2012. ISSN 1939-4586. . URL https://www.molbiolcell.org/doi/10.1091/mbc.e12-05-0400http://www.ncbi.nlm.nih.gov/pubmed/22918946http://www.pubmedcentral.nih.gov/articlerender.fcgi?artid=PMC3459858.
73. Malika Jaquenoud and Matthias Peter. Gic2p May Link Activated Cdc42p to Components Involved in Actin Polarization, Including Bni1p and Bud6p (Aip3p). *Molecular and Cellular Biology*, 20(17):6244–6258, 9 2000. ISSN 0270-7306. . URL https://journals.asm.org/doi/10.1128/MCB.20.17.6244-6258.2000.
74. Yi-Jun Sheu, Beatriz Santos, Nathalie Fortin, Christine Costigan, and Michael Snyder. Spa2p Interacts with Cell Polarity Proteins and Signaling Components Involved in Yeast Cell Morphogenesis. *Molecular and Cellular Biology*, 18(7):4053–4069, 7 1998. ISSN 0270-7306. . URL https://journals.asm.org/doi/10.1128/MCB.18.7.4053http://www.ncbi.nlm.nih.gov/pubmed/9632790http://www.pubmedcentral.nih.gov/articlerender.fcgi?artid=PMC108990.
75. Anita T Layton, Natasha S Savage, Audrey S Howell, Susheela Y Carroll, David G Drubin, and Daniel J Lew. Modeling Vesicle Traffic Reveals Unexpected Consequences for Cdc42p-Mediated Polarity Establishment. *Current Biology*, 21(3):184–194, 2 2011. ISSN 0960-9822. .

76. Natasha S Savage, Anita T Layton, and Daniel J Lew. Mechanistic mathematical model of polarity in yeast. *Molecular Biology of the Cell*, 23(10):1998–2013, 2012. ISSN 1059-1524. . URL https://www.molbiolcell.org/doi/10.1091/mbc.e11-10-0837http://www.ncbi.nlm.nih.gov/pubmed/22438587http://www.pubmedcentral.nih.gov/articlerender.fcgi?artid=PMC3350562.
77. Benjamin Woods, Helen Lai, Chi Fang Wu, Trevin R Zyla, Natasha S Savage, and Daniel J Lew. Parallel Actin-Independent Recycling Pathways Polarize Cdc42 in Budding Yeast. *Current Biology*, 26(16):2114–2126, 8 2016. ISSN 09609822. . URL http://www.cell.com/article/S0960982216306881/fulltexthttp://www.cell.com/article/S0960982216306881/abstracthttps://www.cell.com/current-biology/abstract/S0960-9822(16)30688-1.
78. Bruce L Goode, Julian A Eskin, and Beverly Wendland. Actin and Endocytosis in Budding Yeast. *Genetics*, 199(2):315–358, 2 2015. ISSN 1943-2631. . URL https://academic.oup.com/genetics/article/199/2/315/5935817.
79. Mithilesh Mishra, Junqi Huang, and Mohan K Balasubramanian. The yeast actin cytoskeleton. *FEMS Microbiology Reviews*, 38(2):213–227, 2014. ISSN 0168-6445. . URL https://academic.oup.com/femsre/article/38/2/213/497279.
80. Jessica L D'Agostino and Bruce L Goode. Dissection of Arp2/3 Complex Actin Nucleation Mechanism and Distinct Roles for Its Nucleation-Promoting Factors in Saccharomyces cerevisiae. *Genetics*, 171(1):35–47, 9 2005. ISSN 1943-2631. . URL /pmc/articles/PMC1456526//pmc/articles/PMC1456526/?report=abstracthttps://www.ncbi.nlm.nih.gov/pmc/articles/PMC1456526/https://academic.oup.com/genetics/article/171/1/35/6060516.
81. Terry Lechler, Gudrun A Jonsdottir, Saskia K Klee, David Pellman, and Rong Li. A two-tiered mechanism by which Cdc42 controls the localization and activation of an Arp2/3-activating motor complex in yeast. *Journal of Cell Biology*, 155(2):261–270, 2001. ISSN 0021-9525. . URL http://www.jcb.org/cgi/doi/10.1083/jcb.200104094.
82. Javier E Irazoqui, Audrey S Howell, Chandra L Theesfeld, and Daniel J Lew. Opposing Roles for Actin in Cdc42p Polarization. *Molecular Biology of the Cell*, 16(3):1296–1304, 3 2005. ISSN 1059-1524. . URL https://www.molbiolcell.org/doi/10.1091/mbc.e04-05-0430http://www.ncbi.nlm.nih.gov/pubmed/15616194http://www.pubmedcentral.nih.gov/articlerender.fcgi?artid=PMC551493.
83. Kathryn P. Harris and Ulrich Tepass. Cdc42 and Vesicle Trafficking in Polarized Cells. *Traffic*, 11(10):1272–1279, 2010. ISSN 13989219. .
84. Mini Jose, Sylvain Tollis, Deepak Nair, Jean-Baptiste Sibarita, and Derek McCusker. Robust polarity establishment occurs via an endocytosis-based cortical corralling mechanism. *Journal of Cell Biology*, 200(4):407–418, 2 2013. ISSN 1540-8140. . URL http://www.ncbi.nlm.nih.gov/pubmed/23401000http://www.pubmedcentral.nih.gov/articlerender.fcgi?artid=PMC3575534https://rupress.org/jcb/article/200/4/407/37215/Robust-polarity-establishment-occurs-via-an.
85. Kyoungtae Kim, Atsuko Yamashita, Martin A. Wear, Yuichiro Maéda, and John A. Cooper. Capping protein binding to actin in yeast biochemical mechanism and physiological relevance. *Journal of Cell Biology*, 164(4):567–580, 2 2004. ISSN 0021-9525. . URL http://www.jcb.org/cgi/doi/10.1083/jcb.200308061.
86. Michael E Young, John A Cooper, and Paul C Bridgman. Yeast actin patches are networks of branched actin filaments. *Journal of Cell Biology*, 166(5):629–635, 8 2004. ISSN 0021-9525. . URL http://www.jcb.org/cgi/doi/10.1083/jcb.200404159.
87. Omar Quintero-Monzon, Avital A Rodal, Boris Strokopytov, Steven C Almo, and Bruce L Goode. Structural and Functional Dissection of the Abp1 ADFH Actin-binding Domain Reveals Versatile In Vivo Adapter Functions. *Molecular Biology of the Cell*, 16(7):3128–3139, 7 2005. ISSN 1059-1524. . URL https://www.molbiolcell.org/doi/10.1091/mbc.e05-01-0059http://www.ncbi.nlm.nih.gov/pubmed/15872087http://www.pubmedcentral.nih.gov/articlerender.fcgi?artid=PMC1165398.
88. Elodie Caudal, Anne Friedrich, Arthur Jallet, Marion Garin, Jing Hou, and Joseph Schacherer. Loss-of-function mutation survey revealed that genes with background-dependent fitness are rare and functionally related in yeast. *Proceedings of the National Academy of Sciences*, 119(37):e2204206119, 9 2022. ISSN 0027-8424. . URL https://www.pnas.org/doi/abs/10.1073/pnas.2204206119https://pnas.org/doi/full/10.1073/pnas.2204206119.
89. Martin N. Mullis, Takeshi Matsui, Rachel Schell, Ryan Foree, and Ian M. Ehrenreich. The complex underpinnings of genetic background effects. *Nature Communications*, 9(1):3548, 9 2018. ISSN 2041-1723. . URL https://www.nature.com/articles/s41467-018-06023-5.
90. Michael Costanzo, Jing Hou, Vincent Messier, Justin Nelson, Mahfuzur Rahman, Benjamin VanderSluis, Wen Wang, Carles Pons, Catherine Ross, Matej Ušaj, Bryan-Joseph San Luis, Emira Shuteriqi, Elizabeth N Koch, Patrick Aloy, Chad L Myers, Charles Boone, and Brenda Andrews. Environmental robustness of the global yeast genetic interaction network. *Science*, 372(6542), 2021. ISSN 0036-8075. . URL https://doi.org/10.1126/science.abf8424https://www.science.org/doi/10.1126/science.abf8424.
91. Christian von Mering, Roland Krause, Berend Snel, Michael Cornell, Stephen G. Oliver, Stanley Fields, and Peer Bork. Comparative assessment of large-scale data sets of protein–protein interactions. *Nature*, 417(6887):399–403, 5 2002. ISSN 0028-0836. . URL https://www.nature.com/articles/nature750http://www.nature.com/articles/nature750.
92. Jesse Gillis, Sara Ballouz, and Paul Pavlidis. Bias tradeoffs in the creation and analysis of protein–protein interaction networks. *Journal of Proteomics*, 100:44–54, 4 2014. ISSN 18743919. . URL /pmc/articles/PMC3972268//pmc/articles/PMC3972268/?report=abstracthttps://www.ncbi.nlm.nih.gov/pmc/articles/PMC3972268/https://linkinghub.elsevier.com/retrieve/pii/S1874391914000384.
93. Teunis J P Van Dam and Berend Snel. Protein Complex Evolution Does Not Involve Extensive Network Rewiring. *PLOS Computational Biology*, 4(7):e1000132, 2008. ISSN 1553-7358. . URL https://journals.plos.org/ploscompbiol/article?id=10.1371/journal.pcbi.1000132.
94. Marco Y. Hein, Nina C. Hubner, Ina Poser, Jürgen Cox, Nagarjuna Nagaraj, Yusuke Toyoda, Igor A. Gak, Ina Weisswange, Jörg Mansfeld, Frank Buchholz, Anthony A. Hyman, and Matthias Mann. A Human Interactome in Three Quantitative Dimensions Organized by Stoichiometries and Abundances. *Cell*, 163(3):712–723, 10 2015. ISSN 00928674. . URL https://linkinghub.elsevier.com/retrieve/pii/S0092867415012702.
95. José I Rojas Echenique, Sergey Kryazhimskiy, Alex N Nguyen Ba, and Michael M Desai. Modular epistasis and the compensatory evolution of gene deletion mutants. *PLOS Genetics*, 15(2):e1007958, 2 2019. ISSN 1553-7404. . URL https://journals.plos.org/plosgenetics/article?id=10.1371/journal.pgen.1007958.
96. Russell M Gordley, Lukasz J Bugaj, and Wendell A Lim. Modular engineering of cellular signaling proteins and networks. *Current Opinion in Structural Biology*, 39:106–114, 8 2016. ISSN 0959440X. . URL https://linkinghub.elsevier.com/retrieve/pii/S0959440X16300690.
97. W. R. Harcombe, R. Springman, and J. J. Bull. Compensatory evolution for a gene deletion is not limited to its immediate functional network. *BMC Evolutionary Biology*, 9(1):1–11, 5 2009. ISSN 14712148. . URL https://bmcecolevol.biomedcentral.com/articles/10.1186/1471-2148-9-106.
98. Júlia Domingo, Pablo Baeza-Centurion, and Ben Lehner. The Causes and Consequences of Genetic Interactions (Epistasis). *Annual Review of Genomics and Human Genetics*, 20(1):433–460, 8 2019. ISSN 1527-8204. . URL https://www.annualreviews.org/doi/abs/10.1146/annurev-genom-083118-014857https://www.annualreviews.org/doi/10.1146/annurev-genom-083118-014857.
99. Ruth Nussinov, Chung-Jung Tsai, and Hyunbum Jang. Protein ensembles link genotype to phenotype. *PLOS Computational Biology*, 15(6):e1006648, 6 2019. ISSN 1553-7358. . URL https://dx.plos.org/10.1371/journal.pcbi.1006648.
100. Ruth Nussinov, Yonglan Liu, Wengang Zhang, and Hyunbum Jang. Protein conformational ensembles in function: roles and mechanisms. *RSC Chemical Biology*, 4(11):850–864, 2023. ISSN 2633-0679. . URL http://xlink.rsc.org/?DOI=D3CB00114H.
101. Petra Schwille and Béla P. Frohn. Hidden protein functions and what they may teach us. *Trends in Cell Biology*, 32(2):102–109, 2 2022. ISSN 09628924. . URL https://linkinghub.elsevier.com/retrieve/pii/S0962892421001859.
102. David D Boehr, Ruth Nussinov, and Peter E Wright. The role of dynamic conformational ensembles in biomolecular recognition. *Nature Chemical Biology*, 5(11):789–796, 11 2009. ISSN 1552-4450. . URL https://www.nature.com/articles/nchembio.232.
103. Cristina Guijarro-Clarke, Peter W. H. Holland, and Jordi Paps. Widespread patterns of gene loss in the evolution of the animal kingdom. *Nature Ecology & Evolution*, 4(4):519–523, 2 2020. ISSN 2397-334X. . URL https://www.nature.com/articles/s41559-020-1129-2.
104. Cristian Cañestro and John H. Postlethwait. Development of a chordate anterior–posterior axis without classical retinoic acid signaling. *Developmental Biology*, 305(2):522–538, 5 2007. ISSN 00121606. . URL https://linkinghub.elsevier.com/retrieve/pii/S0012160607001492.
105. Andrew W Murray. Can gene-inactivating mutations lead to evolutionary novelty? *Current Biology*, 30(10):R465–R471, 2020. ISSN 0960-9822. . URL http://www.cell.com/article/S0960982220304796/fulltexthttp://www.cell.com/article/S0960982220304796/abstracthttps://www.cell.com/current-biology/abstract/S0960-9822(20)30479-6.
106. James E. Dicarlo, Julie E. Norville, Prashant Mali, Xavier Rios, John Aach, and George M. Church. Genome engineering in Saccharomyces cerevisiae using CRISPR-Cas systems. *Nucleic Acids Research*, 41(7):4336–4343, 4 2013. ISSN 0305-1048. . URL https://academic.oup.com/nar/article/41/7/4336/1075252.
107. R. Daniel Gietz and Robert H. Schiestl. High-efficiency yeast transformation using the LiAc/SS carrier DNA/PEG method. *Nature Protocols*, 2(1):31–34, 1 2007. ISSN 1754-2189. . URL https://www.nature.com/articles/nprot.2007.13http://www.nature.com/articles/nprot.2007.13.
108. Robert Mans, Harmen M. van Rossum, Melanie Wijsman, Antoon Backx, Niels G.A. Kuijpers, Marcel van den Broek, Pascale Daran-Lapujade, Jack T. Pronk, Antonius J.A. van Maris, and Jean-Marc G. Daran. CRISPR/Cas9: a molecular Swiss army knife for simultaneous introduction of multiple genetic modifications in Saccharomyces cerevisiae. *FEMS Yeast Research*, 15(2):1–21, 3 2015. ISSN 1567-1356. . URL http://academic.oup.com/femsyr/article/doi/10.1093/femsyr/fov004/536897/CRISPRCas9-a-molecular-Swiss-army-knife-for.
109. Kornel Labun, Tessa G Montague, Maximilian Krause, Yamila N Torres Cleuren, Håkon Tjeldnes, and Eivind Valen. CHOPCHOP v3: expanding the CRISPR web toolbox beyond genome editing. *Nucleic Acids Research*, 47(W1):W171–W174, 7 2019. ISSN 0305-1048. . URL https://academic.oup.com/nar/article/47/W1/W171/5491735.
110. Agnès H Michel, Sabine van Schie, Andreas Mosbach, Gabriel Scalliet, and Benoît Kornmann. Exploiting homologous recombination increases SATAY efficiency for loss- and gain-of-function screening. *bioRxiv*, page 866483, 12 2019. . URL https://www.biorxiv.org/content/10.1101/866483v1https://www.biorxiv.org/content/10.1101/866483v1.abstract.
111. Agnès H Michel, Riko Hatakeyama, Philipp Kimmig, Meret Arter, Matthias Peter, Joao Matos, Claudio De Virgilio, and Benoît Kornmann. Functional mapping of yeast genomes by saturated transposition. *eLife*, 6, 5 2017. ISSN 2050-084X. . URL https://elifesciences.org/articles/23570.
112. Agnès H Michel and Benoît Kornmann. SAturated Transposon Analysis in Yeast (SATAY) for Deep Functional Mapping of Yeast Genomes. In *Methods in molecular biology (Clifton, N.J.)*, volume 2477, pages 349–379. Humana Press Inc., 2022. . URL https://link.springer.com/protocol/10.1007/978-1-0716-2257-5_20http://www.ncbi.nlm.nih.gov/pubmed/35524127https://link.springer.com/10.1007/978-1-0716-2257-5_20.
113. Brian Bushnell, Jonathan Rood, and Esther Singer. BBMerge – Accurate paired shotgun read merging via overlap. *PLOS ONE*, 12(10):e0185056, 10 2017. ISSN 1932-6203. .
114. Leila Iñigo de la Cruz, Gregory van Beek, and Maurits Kok. transposonmapper, 1 2022. URL https://doi.org/10.5281/zenodo.5903081#.Y6L8bYdxJII.mendeley.

115. Pauli Virtanen, Ralf Gommers, Travis E Oliphant, Matt Haberland, Tyler Reddy, David Cournapeau, Evgeni Burovski, Pearu Peterson, Warren Weckesser, Jonathan Bright, Stéfan J van der Walt, Matthew Brett, Joshua Wilson, K Jarrod Millman, Nikolay Mayorov, Andrew R J Nelson, Eric Jones, Robert Kern, Eric Larson, C J Carey, İlhan Polat, Yu Feng, Eric W Moore, Jake VanderPlas, Denis Laxalde, Josef Perktold, Robert Cimrman, Ian Henriksen, E A Quintero, Charles R Harris, Anne M Archibald, Antônio H Ribeiro, Fabian Pedregosa, Paul van Mulbregt, Aditya Vijaykumar, Alessandro Pietro Bardelli, Alex Rothberg, Andreas Hilboll, Andreas Kloeckner, Anthony Scopatz, Antony Lee, Ariel Rokem, C Nathan Woods, Chad Fulton, Charles Masson, Christian Häggström, Clark Fitzgerald, David A Nicholson, David R Hagen, Dmitrii V Pasechnik, Emanuele Olivetti, Eric Martin, Eric Wieser, Fabrice Silva, Felix Lenders, Florian Wilhelm, G Young, Gavin A Price, Gert-Ludwig Ingold, Gregory E Allen, Gregory R Lee, Hervé Audren, Irvin Probst, Jörg P Dietrich, Jacob Silterra, James T Webber, Janko Slavič, Joel Nothman, Johannes Buchner, Johannes Kulick, Johannes L Schönberger, José Vinícius de Miranda Cardoso, Joscha Reimer, Joseph Harrington, Juan Luis Cano Rodríguez, Juan Nunez-Iglesias, Justin Kuczynski, Kevin Tritz, Martin Thoma, Matthew Newville, Matthias Kümmerer, Maximilian Bolingbroke, Michael Tartre, Mikhail Pak, Nathaniel J Smith, Nikolai Nowaczyk, Nikolay Shebanov, Oleksandr Pavlyk, Per A Brodtkorb, Perry Lee, Robert T McGibbon, Roman Feldbauer, Sam Lewis, Sam Tygier, Scott Sievert, Sebastiano Vigna, Stefan Peterson, Surhud More, Tadeusz Pudlik, Takuya Oshima, Thomas J Pingel, Thomas P Robitaille, Thomas Spura, Thouis R Jones, Tim Cera, Tim Leslie, Tiziano Zito, Tom Krauss, Utkarsh Upadhyay, Yaroslav O Halchenko, and Yoshiki Vázquez-Baeza. SciPy 1.0: fundamental algorithms for scientific computing in Python. *Nature Methods*, 17(3):261–272, 2020. ISSN 1548-7091. . URL https://www.nature.com/articles/s41592-019-0686-2http://www.nature.com/articles/s41592-019-0686-2.

116. Michael A DeJesus, Chaitra Ambadipudi, Richard Baker, Christopher Sassetti, and Thomas R Ioerger. TRANSIT - A Software Tool for Himar1 TnSeq Analysis. *PLOS Computational Biology*, 11(10): e1004401, 2015. ISSN 1553-7358. . URL https://journals.plos.org/ploscompbiol/article?id=10.1371/journal.pcbi.1004401https://dx.plos.org/10.1371/journal.pcbi.1004401.

117. J. Michael Cherry, Eurie L. Hong, Craig Amundsen, Rama Balakrishnan, Gail Binkley, Esther T. Chan, Karen R. Christie, Maria C. Costanzo, Selina S. Dwight, Stacia R. Engel, Dianna G. Fisk, Jodi E. Hirschman, Benjamin C. Hitz, Kalpana Karra, Cynthia J. Krieger, Stuart R. Miyasato, Rob S. Nash, Julie Park, Marek S. Skrzypek, Matt Simison, Shuai Weng, and Edith D. Wong. Saccharomyces Genome Database: the genomics resource of budding yeast. *Nucleic Acids Research*, 40(D1):D700–D705, 1 2012. ISSN 0305-1048. . URL https://academic.oup.com/nar/article/40/D1/D700/2902744https://academic.oup.com/nar/article-lookup/doi/10.1093/nar/gkr1029.

118. Paul Shannon, Andrew Markiel, Owen Ozier, Nitin S. Baliga, Jonathan T. Wang, Daniel Ramage, Nada Amin, Beno Schwikowski, and Trey Ideker. Cytoscape: A software Environment for integrated models of biomolecular interaction networks. *Genome Research*, 13(11):2498–2504, 11 2003. ISSN 10889051. . URL http://genome.cshlp.org/lookup/doi/10.1101/gr.1239303.

119. Aric A Hagberg, Daniel A Schult, and Pieter J Swart. Exploring Network Structure, Dynamics, and Function using NetworkX. In Gaël Varoquaux, Travis Vaught, and Jarrod Millman, editors, *Proceedings of the 7th Python in Science Conference*, pages 11–15, Pasadena, CA USA, 2008.

120. Michael A. DeJesus and Thomas R. Ioerger. Normalization of transposon-mutant library sequencing datasets to improve identification of conditionally essential genes. *Journal of Bioinformatics and Computational Biology*, 14(03):1642004, 6 2016. ISSN 0219-7200. . URL https://www.worldscientific.com/doi/abs/10.1142/S021972001642004X.

121. Michael A DeJesus and Thomas R Ioerger. A Hidden Markov Model for identifying essential and growth-defect regions in bacterial genomes from transposon insertion sequencing data. *BMC Bioinformatics*, 14(1):303, 12 2013. ISSN 1471-2105. . URL https://bmcbioinformatics.biomedcentral.com/articles/10.1186/1471-2105-14-303.

122. Simon Anders and Wolfgang Huber. Differential expression analysis for sequence count data. *Genome Biology*, 11(10):R106, 10 2010. ISSN 1474-760X. . URL https://genomebiology.biomedcentral.com/articles/10.1186/gb-2010-11-10-r106http://www.ncbi.nlm.nih.gov/pubmed/20979621http://www.pubmedcentral.nih.gov/articlerender.fcgi?artid=PMC3218662.

123. Mark D Robinson and Alicia Oshlack. A scaling normalization method for differential expression analysis of RNA-seq data. *Genome Biology*, 11(3):R25, 2010. ISSN 1465-6906. . URL https://genomebiology.biomedcentral.com/articles/10.1186/gb-2010-11-3-r25http://www.ncbi.nlm.nih.gov/pubmed/20196867http://www.pubmedcentral.nih.gov/articlerender.fcgi?artid=PMC2864565http://genomebiology.biomedcentral.com/articles/10.1186/gb-2010-11-3.

6. Supplement

A. Read count correction and normalization procedure. The benefit of including read counts in our metric to identify changes in the fitness effect of gene disruptions across genetic backgrounds is that it allows for a more sensitive analysis than those based on insertion counts. For example, a gene may have a negligible difference in insertion counts between two genetic backgrounds if the change in gene disruption tolerance is not so drastic that it causes a large number of mutants to fall below the detection level in one of the two backgrounds. However, if a significant difference in gene disruption tolerance truly exists, we would expect that the read counts associated with each insertion site (which reflect mutant abundance) will be lower in one of the two strains. Thus, extending the analysis from a binary assessment of the occupancy of insertion sites to a gradual scale based on read counts can uncover differences that would otherwise remain undetected. However, a drawback is that read counts tend to be more variable between replicate experiments than insertion counts, often owing to read count spikes caused by technical and biological artifacts (120). This increased noise level can hinder the desired increase of sensitivity of the analysis. In addition, spikes in the read counts can significantly skew the read count distribution. This means that the small subset of insertion sites with an artificially high read count will strongly affect methods that aim to correct differences in sequencing depth between libraries by a linear transformation of the total read count.

To address these issues, we implemented the Beta-Geometric correction (BGC) method developed by DeJesus and Ioerger (121). This method is based on the observation that read count distributions obtained from transposon insertion sequencing (TIS) experiments resemble a geometric distribution where most insertion sites have a low read count, while only few sites contain many reads. During the BGC correction procedure, the quantiles of the empirical read count distribution are adjusted to match the quantiles of a fitted 'ideal' geometric distribution. To allow for greater flexibility of the fit, this ideal distribution is implemented as a mixture of geometric distributions with a Beta prior on the probability parameter. In practice, this procedure corrects for the 'skew' in the empirical read count distribution by suppressing spikes while inflating the insertion sites that have a low read count. The results in figure S1 show that the application of this procedure greatly improves the correlation between replicate datasets (figure S1b) compared to uncorrected datasets (figure S1a). Lastly, after applying the BGC correction, we normalized for differences in sequencing depth and library complexity across datasets using the median of ratios normalization (122, 123). In summary, the geometric mean across all samples was calculated for each gene:

$$\bar{X}_g = \exp \frac{1}{n} \cdot \sum_{a}^{n} \ln \left(R_{g,a}\right)). \qquad [1]$$

Where $\bar{X}_g$ is the geometric mean of the read counts mapping to gene g, n is the total number of datasets and $R_{g,a}$ is the number of reads that map to gene g in dataset a. Next, the ratio of the total read count to the geometric mean $\bar{X}_g$ was determined for each sample and the sample-specific normalization factor was taken to be the median of these ratios across all genes:

$$S_a = \text{median}(\frac{R_{g,a}}{\bar{X}_g}) \ , \text{ for all } a \in G \qquad [2]$$

With S_a the normalization factor for dataset a and G is the complete set of annotated genes used in this chapter. Finally, the read counts were linearly scaled by the normalization factor S_a:

$$R_{g,a,\text{norm}} = \frac{R_{g,a}}{S_a}. \qquad [3]$$

B. Supplemental figures.

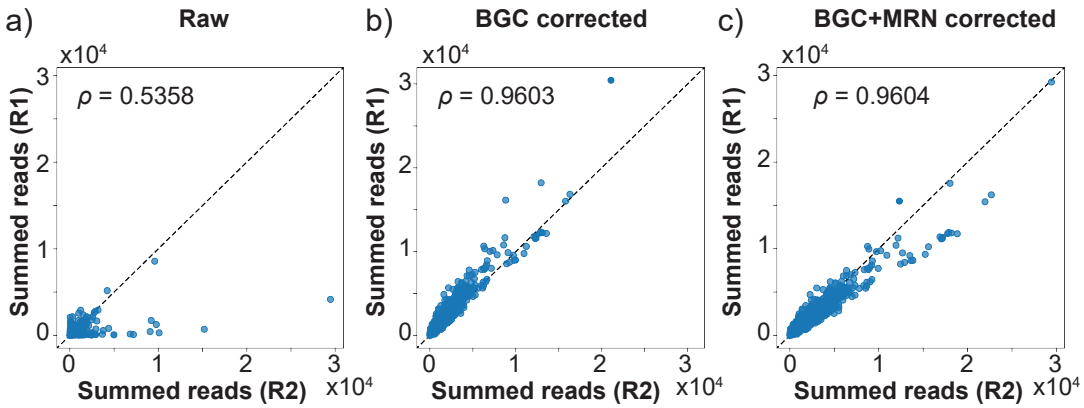

Fig. S1. Normalization procedure increases correlation in the summed read counts per gene between replicate experiments. In order to improve the correlation between replicate datasets derived from the same genetic background, the datasets are first aligned with their best fitting Beta-Geometric distribution (panel (a) to panel (b)) to correct for spikes in read counts, followed by a median of ratios normalization to account for differences in sequencing depth (panel (b) to panel (c)). In each panel, the value of Pearson's correlation coefficient (ρ) is shown.

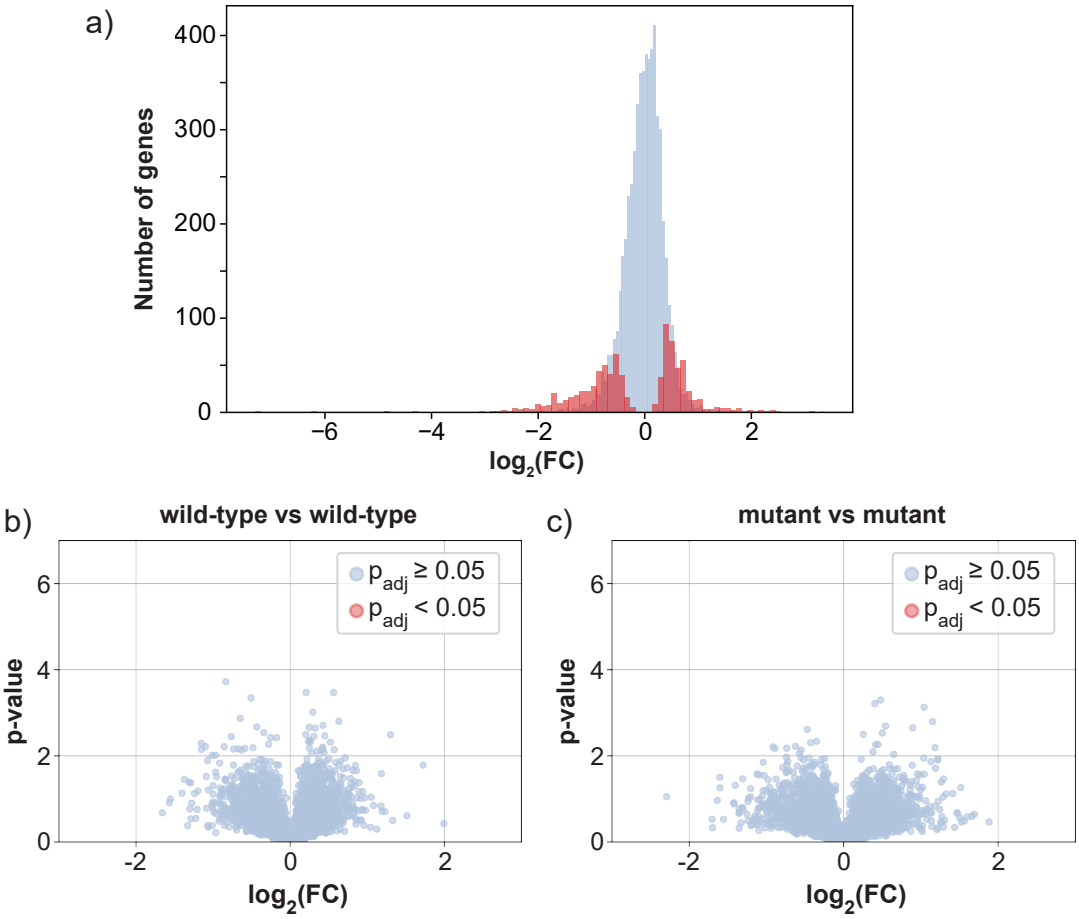

Fig. S2. Validity of the geneset that is identified as having differential fitness between the wild-type strain and the polarity mutant. (**a**) Significant genes have a larger effect size. Histogram of the $\log_2$-fold changes shown in figure 2. The plot shows that genes that are flagged to have a statistically significant difference between the two genetic backgrounds (red bars) typically occurs for larger fold-changes. (**b**) Comparing transposon mutagenesis libraries obtained from the same genetic background yields no significant differences in gene fitness. Volcano plots are shown for comparisons between wild-type and mutant datasets. The replicate datasets of each genetic background (6 in total) were split and compared 3 vs. 3. For both our wild-type strain and from our polarity mutant, no false positives are found at a significance threshold of $\mathrm{p_{adj}} < 0.05$.

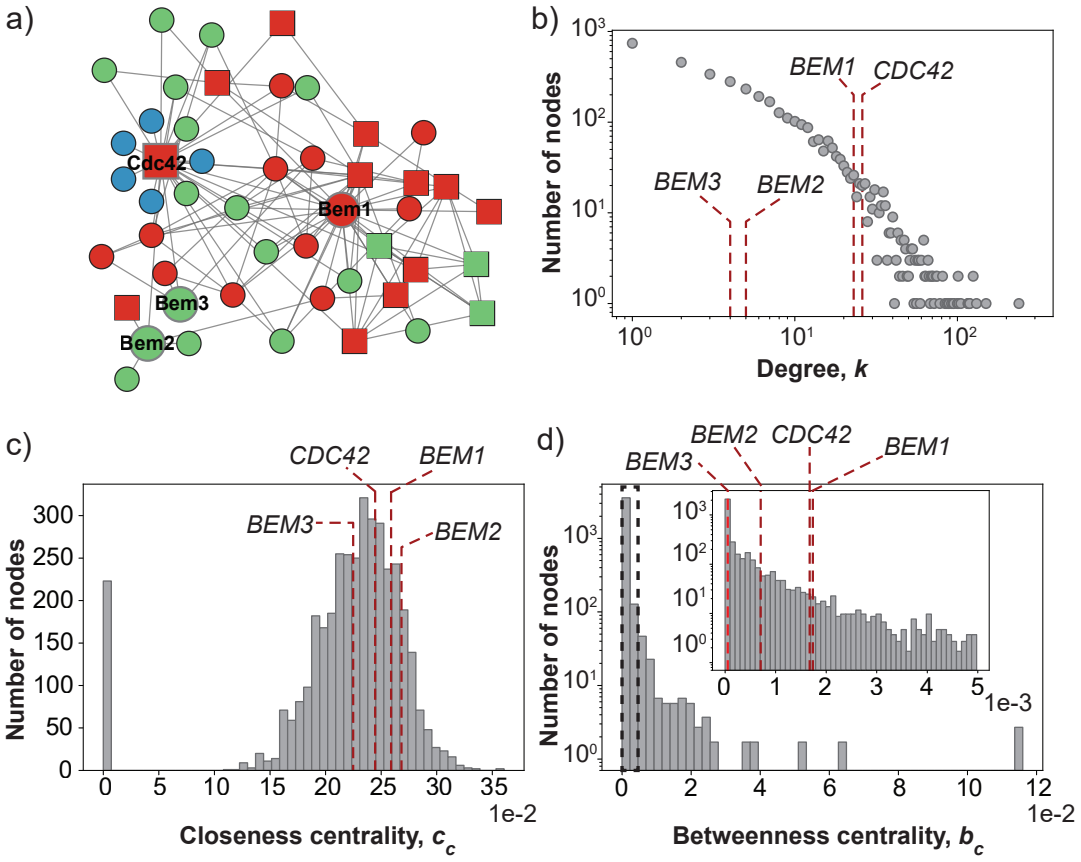

Fig. S3. Properties of the constructed protein-protein interaction network. (**a**) Sub-graph of of the protein-protein interaction network for Cdc42, Bem1, Bem2 and Bem3 and their first neighbours. Nodes are colored according to their degree k in the complete PPI network (figure 3a). Blue: $k \leq 3$, green: $4 \leq k \leq 10$, red: $k > 10$. Proteins that have previously been annotated as essential are shown as squares, non-essential proteins are shown as circles. (**b**) The degree centrality of the nodes in the complete PPI network. The degree distribution shows the typical sub-linearity of PPI networks in biology when plotted on a log-log scale. (**c**) The closeness centrality distribution of the PPI network. (**d**) the betweenness centrality distribution of the PPI network. In the panels **c**-**d**, the degree values are indicated for two polarity proteins that have a strong negative effect on fitness when deleted (Bem1 and Cdc42) and for two polarity proteins that have a moderate to weak negative effect (Bem3 and Bem2). With respect to degree and betweenness, proteins with a similar gene fitness lie in proximity of each other on the distributions. For the closeness distribution, we find no relation with gene fitness.

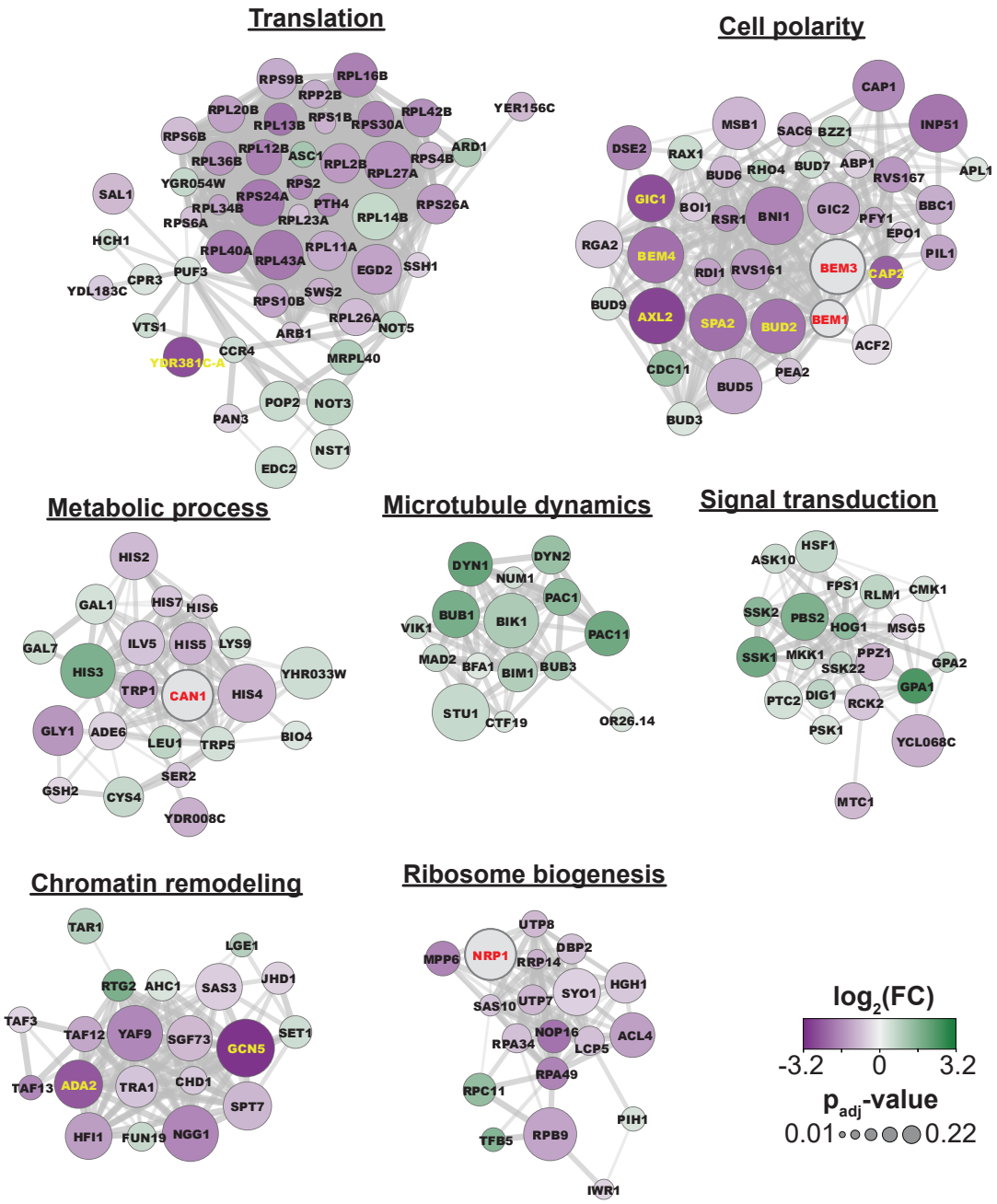

Fig. S4. Zoom-in of the seven largest clusters identified in our functional association network by the Markov clustering algorithm The biological process gene ontology enrichment is shown above each cluster.

C. Supplemental tables.

Table S1. Liquid media used for SATAY library generation. YNB: Yeast Nitrogen Base. CSM: Complete Supplement Mixture. Ura: Uracil. Ade: Adenine

Step	Media	Components
Preculture	SD-Ura+0.2% Glucose +2% Raffinose	• YNB w/o Amino Acids (6.8 g/L) • CSM -Ura (0.77 g/L) • Glucose (2 g/L) • Raffinose (20 g/L) • Adenine (20 mg/L)
Induction	SD-Ura+2% Galactose	• YNB w/o Amino Acids (6.8 g/L) • CSM -Ura (0.77 g/L) • Galactose (20 g/L) • Adenine (20 mg/L)
Reseed	SD-Ade+2% Glucose	• YNB w/o Amino Acids (6.8 g/L) • CSM -Ade (0.78 g/L) • Glucose (20 g/L)

Table S2. List of used primers

#	Name	Barcode	Sequence (5'-3')
1	HT50_688_minidsSEQ1210	HT50	GCC ACA TAT TTA CCG ACC GTT ACC GAC CGT TTT CAT CCC TA
2	E2_HT48_MiniDS_RV	HT48	AGG TCA GTC ACA TGG TTA GGA CGC AGA GCT GAA ACG AAA ACG AAC GGG ATA AA
3	HT60_688_minidsSEQ1210	HT60	TAG GAT GAT TTA CCG ACC GTT ACC GAC CGT TTT CAT CCC TA
4	E2_HT49_MiniDS_RV	HT49	AGG TCA GTC ACA TGG TTA GGA CGC AGA TAG ACA ACG AAA ACG AAC GGG ATA AA